THESIS FOR THE DEGREE OF LICENTIATE OF ENGINEERING

Optical Mapping of Bacterial Plasmids

Method Development and Applications

VILHELM MÜLLER

Department of Biology and Biological Engineering

CHALMERS UNIVERSITY OF TECHNOLOGY

Gothenburg, Sweden 2017

Optical Mapping of Bacterial Plasmids
Method Development and Applications
VILHELM MÜLLER

Department of Biology and Biological Engineering
Chalmers University of Technology
SE-412 96 Gothenburg
Sweden
Telephone + 46 (0)31-772 1000

Cover:
Schematic illustration of plasmid DNA molecules labeled with the fluorescent dye YOYO-1 (green) and the AT-selective molecule netropsin (gray), before subsequent confinement inside nanochannels. Red scissors illustrate a Cas9 enzyme targeting a resistance gene (red) located on the plasmid molecules.

Printed by Chalmers Reproservice
Gothenburg, Sweden 2017

Optical Mapping of Bacterial Plasmids

Method Development and Applications

VILHELM MÜLLER

Department of Biology and Biological Engineering
Chalmers University of Technology

Abstract

Bacteria that have acquired resistance to antibiotics represent one of the largest threats to human health and modern health care. The genes encoding resistance are frequently spread via the transfer of plasmids, which are circular double stranded DNA molecules separate from the chromosomal DNA of the bacteria. The increasing prevalence of resistant bacteria, in combination with the absence of new major discoveries of antimicrobial drugs, means that health care could soon be entering a "post-antibiotic era". Besides developing new drugs, methods capable of rapidly detecting bacteria that have acquired resistance to antibiotics are of paramount importance for clinical point of care applications.

In this Thesis, the development of an assay for rapid plasmid characterization is described. The method is based on optical DNA mapping using competitive binding of the fluorophore YOYO-1 and the sequence-specific, non-fluorescent, molecule netropsin, to DNA. The fluorescently labeled DNA is stretched in nanofluidic channels and imaged using fluorescence microscopy, enabling coarse-grained sequence information to be read from the intact plasmid at the single plasmid level. Additionally, an approach for gene detection on individual plasmids is described, combining the CRISPR/Cas9 system with optical DNA mapping.

The results demonstrate how the assay can be used to obtain the number of different plasmids in a sample, the size of each plasmid, an optical barcode for tracing and identification, as well as information about which plasmid that carries a specific (resistance) gene. Overall, the assay shows great potential as a first step of plasmid characterization in point of care diagnostics.

Keywords: plasmids, nanofluidics, antibiotic resistance, DNA, single-molecule, optical mapping, competitive binding, CRISPR/Cas9, fluorescence microscopy.

List of Publications

This Thesis is based on the following papers, referred to in the text by Roman numerals:

I. Rapid identification of intact bacterial resistance plasmids via optical mapping of single DNA molecules
Lena K. Nyberg, Saair Quaderi, Gustav Emilsson, Nahid Karami, Erik Lagerstedt, Vilhelm Müller, Charleston Noble, Susanna Hammarberg, Adam N. Nilsson, Fei Sjöberg, Joachim Fritzsche, Erik Kristiansson, Linus Sandegren, Tobias Ambjörnsson and Fredrik Westerlund
Scientific Reports, **2016**, 6, 30410

II. Rapid tracing of resistance plasmids in a nosocomial outbreak using optical DNA mapping
Vilhelm Müller, Nahid Karami, Lena K. Nyberg, Christoffer Pichler, Paola C. Torche Pedreschi, Saair Quaderi, Joachim Fritzsche, Tobias Ambjörnsson, Christina Åhrén and Fredrik Westerlund
ACS Infectious Disease, **2016**, 2, 322-328

III. Direct identification of antibiotic resistance genes on single plasmid molecules using CRISPR/Cas9 in combination with optical DNA mapping
Vilhelm Müller, Fredrika Rajer, Karolin Frykholm, Lena K. Nyberg, Saair Quaderi, Joachim Fritzsche, Erik Kristiansson, Tobias Ambjörnsson, Linus Sandegren and Fredrik Westerlund
Scientific Reports, **2016**, 6, 37938

Contribution Report

I. Performed part of the experiments and the data analysis. Contributed in writing the paper and in the conceptual design of the data analysis software.

II. Planned and performed all the nanofluidic experiments and analyzed all the data. Contributed in the conceptual design of the data analysis software. Wrote the paper together with FW.

III. Developed the assay together with FW. Planned and performed the nanofluidic experiments and analyzed all the data. Contributed in the conceptual design of the data analysis software. Wrote the paper together with FW.

Table of Contents

1 Introduction

"A post-antibiotic era—in which common infections and minor injuries can kill—far from being an apocalyptic fantasy, is instead a very real possibility for the 21st century."

– Dr. Keiji Fukuda, World Health Organization, 2014

Almost a century has passed since the ground breaking discovery of penicillin by Fleming (1) in 1928, that paved the way for the first clinical use of antibiotics just over a decade later (2). The discovery of antibiotics is regarded as one of the largest break troughs in medicine and antibiotics are today one of the main foundations of modern health care. However, significant overuse of antibiotics, in combination with the lack of new major discoveries, has led to a situation where bacteria have started to acquire resistance to more or less all effective antibiotics, compromising our ability to treat even common bacterial infections (3, 4).

In order to avoid a post-antibiotic era, there is a need for drastically reducing the use of antibiotics, as well as finding new alternative treatments, either in the form of new antibiotics, or by discovering novel ways to target bacterial infections. Additionally, there

is an urgent need for rapid point-of-care (POC) diagnostics in order to replace the inherently slow (>36 hours) assays that are standard today, based on cultivating the bacteria in the presence of different antibiotics (3, 5). With quick and robust tools for diagnostics, adequate treatment could be administered faster and existing antibiotics could be used more efficiently, allowing to spare the "last resort" antibiotics.

One main reason for the rapid spread of antibiotic resistance is horizontal gene transfer, where genes located on mobile genetic elements, such as plasmids, allow resistance to be spread between different bacterial strains and species (6-8). Existing tools for characterizing plasmids allow to measure plasmid size (9), group plasmids based on specific genes (10), and retrieve the entire deoxyribonucleic (DNA) sequence (11). However, at present, available methods that provide enough information for reliable diagnostics suffer from either being slow or complex and expensive, hampering their use in clinics (5, 12, 13).

The aim of this Thesis is to describe the development of a novel assay for rapid plasmid characterization based on optical DNA mapping. Pioneered by Schwartz et al. (14) almost 25 years ago, optical DNA mapping has proven to be a versatile tool for extracting long range sequence information of DNA at the kilo base pair (kbp) level (15, 16). For the assay described in this Thesis, fluorescently labeled DNA is stretched in nanofluidic channels, and imaged using fluorescence microscopy. This approach enables coarse-grained sequence information to be read from intact plasmids at the single plasmid level. Hence, the assay introduces the possibility to study structural variations without averaging, as well as to avoid the time consuming step of bacterial cultivation before subsequent analysis. The latter is a key stepping stone for rapid POC diagnostics of antibiotic resistance.

This general introduction is followed by two chapters in which theoretical background is provided to some of the main topics related to the presented research (**Chapter 2**), along with a description of the key methodologies used (**Chapter 3**). The original work in this Thesis, which is summarized and discussed in **Chapter 4**, is based on the three appended papers, from here on referred to as **Paper I-III**.

Paper I demonstrates how optical DNA mapping can be used to study intact plasmid DNA molecules. An assay was developed to identify and characterize plasmids with genes encoding antibiotic resistance, by comparing to a database of all available sequenced plasmids. **Paper II** applies and extends the assay presented in **Paper I**,

enabling plasmids extracted directly from clinical isolates originating from a nosocomial outbreak at a neonatal ward at Sahlgrenska University Hospital to be studied. By simultaneously extracting information about the size, as well as the underlying sequence of the investigated plasmids, it was possible to trace plasmids between different bacterial strains, species and even patients. **Paper III** adds to the work in **Paper I** and **Paper II** by introducing a CRISPR/Cas9 based approach for gene targeting, allowing resistance genes to be directly detected from optical DNA maps of single plasmids.

Finally, **Chapter 5** provides some concluding remarks, as well as a discussion about future directions of the research.

2 Background

In this chapter, background information is provided on key topics, relevant for the work presented in the Thesis. First, the DNA molecule is described, with focus on structure and molecular interactions. Moreover, the basics of bacteria, and especially their plasmids, is presented, in combination with available techniques for plasmid characterization. Information is also provided regarding antibiotic resistance, including existing knowledge about bacterial defense and transfer mechanisms. Finally, an introduction to the field of optical DNA mapping is given.

2.1 DNA

During the 20th century, the understanding of deoxyribonucleic acid, DNA, and its role in biological systems started to grow. Avery and co-workers showed in 1944 that DNA, and not proteins as previously supposed, was responsible for inheritance (17). Still, the mechanism of genetic heredity remained a mystery until Watson and Crick published the structure of double stranded DNA (dsDNA) (Figure 1) in 1953 (18), followed by a

suggestion on how genetic material could be replicated and transferred to the next generation (19).

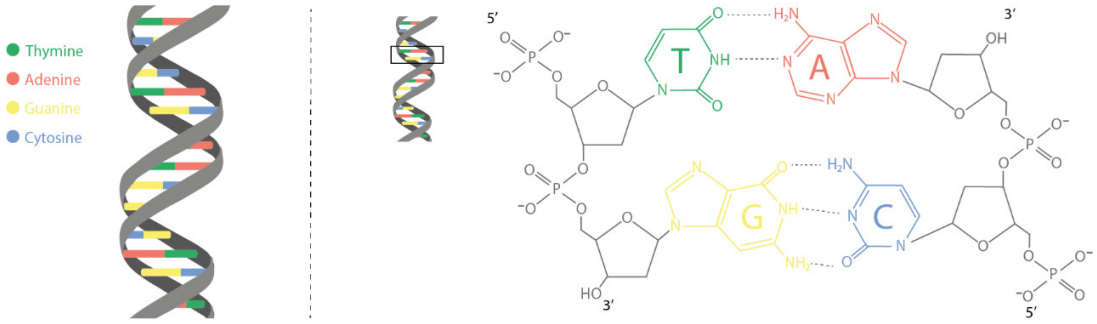

Figure 1: *Molecular structure of DNA. Left: Helical arrangement of the two strands, linked via hydrogen bonding between the DNA bases. Right: Molecular structure of the four different DNA bases, thymine (green), adenine (red), guanine (yellow) and cytosine (blue), with hydrogen bonds displayed as dashed lines. The DNA backbone, consisting of a sugar and a phosphate group, is shown in gray.*

2.1.1 Structure and Biological Function

The structure of DNA can be described as pairs of different nucleotides. A nucleotide consists of three distinct units, a phosphate, a deoxyribose sugar and a nitrogen base. In contrast to the phosphate and deoxyribose sugar, which always are the same, there are four different nitrogen bases that make up the DNA structure, thymine (T), adenine (A), cytosine (C) and guanine (G), where T and C belong to the family of pyrimidines and A and G are purines. Hence, there are four possible nucleotide versions, each containing one of the four different nitrogen bases.

The nucleotides are connected by phosphodiester bonds between the phosphate and sugars, leading to the formation of single stranded DNA (ssDNA). Each nucleotide is associated with its neighbor from the 5′ carbon on the sugar of the first nucleotide, to the 3′ carbon on the subsequent nucleotide. Hence, ssDNA will have an inherent direction. The two DNA strands are in turn connected by hydrogen bonding between the nitrogen

bases to create the double stranded helix, where A base pairs with T by forming two hydrogen bonds, and G with C, forming three bonds (Figure 1). Three different natural forms of DNA are known, commonly denoted A, B and Z. The B form, which is by far the most abundant in nature, has an overall negative charge under physiological conditions and displays a right-handed helix structure, with a twist angle of 36 degrees, and a rise of 0.34 nm, per base pair (bp) (20).

Following the understanding of the DNA structure, the central dogma of molecular biology was revealed (Figure 2), explaining the relationship between DNA, ribonucleic acid (RNA) and proteins (21, 22). Proteins are long chains built up by twenty different amino acids, linked via peptide bonds. The order of these amino acids in each protein is encoded by a triplet of DNA bases, information that is transferred via RNA molecules.

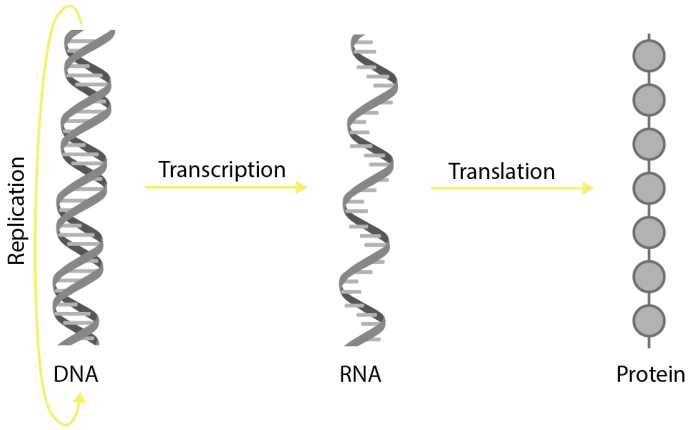

Figure 2: *Schematic illustration of the central dogma of molecular biology. The genetic information stored in DNA, based on the order of the nucleotides, can be replicated, as well as used as a template for RNA generation (transcription). The genetic information, now stored in the form of RNA, is subsequently used to enable protein synthesis via the process of translation.*

2.1.2 Confined DNA

When studying the behavior of DNA at larger length scales, it is not enough to consider only the basic chemistry of the nucleotides. Instead, the DNA can be modeled as a large polymer, built up by many monomeric subunits, characterized by parameters such as size, shape and molar mass. The size and shape of the DNA will depend on the degree of confinement, as well as the surrounding solvent, while the molar mass is determined by the number of monomers.

In order to describe the behavior of DNA, both free in solution and when confined, some basic parameters need to be introduced. The contour length (L) of DNA is defined as the end to end distance of the DNA when fully stretched, and calculated by multiplying the number of monomers, base pairs, with their separation distance. The persistence length (P) of DNA is defined as the length of the unit over which the DNA cannot be bent, and varies with the ionic strength, with an approximate value of 50 nm under physiological conditions (23, 24).

A DNA molecule free in solution will coil in order to minimize its free energy. The size of the coiled DNA can be described by the radius of gyration (R_G), which is a measure of the root mean square distance of the segments to the center of the coil. Additionally, a parameter describing the dimensions of the confining environment is needed. The work in this Thesis is based on confining DNA inside nanochannels, in which the length of the channels are assumed to be infinitely long, while the width and height of the channels are restricted. The dimensions are generally expressed as the average cross section area (D) of the channel width (D_w) and height (D_h), and calculated according to Equation (1)

$$D = \sqrt{D_w \cdot D_h} \tag{1}$$

The degree of extension will depend on the persistence length (P), channel dimensions (D), as well as the radius of gyration (R_G), of the DNA molecule (Figure 3). If the dimensions of the channels are larger than the radius of gyration ($R_G < D$), the DNA will act as when free in solution. If the channel dimensions are smaller than the radius of gyration, but still much larger than the persistence length ($P \ll D < R_G$), the DNA will be weakly confined and can be modeled as a series of non-interacting blobs with diameters similar to the cross section area, as explained by the theory of de Gennes (25).

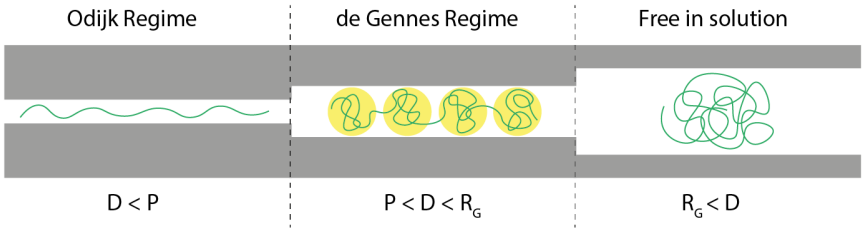

Figure 3: *Illustration of a DNA molecule under different degrees of confinement, where R_G is the radius of gyration and P is the persistence length of the DNA molecule, while D is the average cross section of the confining environment.*

However, if the channels have dimensions smaller than the persistence length ($D < P$), the DNA molecule will behave according to the theory developed by Odijk (26, 27). Here the DNA cannot coil up anymore and movement is restricted to only small undulations (Figure 3). For nanofluidic experiments involving DNA molecules, as for the work in this Thesis, the channel dimensions are similar to the persistence length ($P \leq D$), resulting in that the experiments are conducted in a transition regime in-between the ones described by de Gennes and Odijk, commonly referred to as the extended de Gennes regime (28-32). Notably, the degree of extension in the regimes described by both de Gennes and Odijk is directly proportional to the contour length of the DNA. Hence, sequence specific information positioned X% into the sequence can be observed X% into the nanoconfined DNA molecule.

Finally, since the properties of DNA are sensitive to the concentration of ions, the degree of extension will depend on the ionic strength of the solution. For example, a lower concentration of ions in the solution will provide less shielding for the DNA from its own negatively charged backbone, increasing the stiffness, and thus increase the degree of extension.

2.1.3 DNA Binding Molecules

Due to the versatile chemical and structural properties of DNA, it provides other molecules a variety of possibilities to interact. Figure 4 shows four main ways a molecule, referred to as a ligand, can bind to DNA: external biding, binding to the minor or major groove of the DNA helix, and intercalation between the DNA base pairs. External binding

is facilitated by electrostatic interactions between a positively charged ligand and the negatively charged DNA backbone. Groove binders, on the other hand, rely on forming hydrogen bonds with the exposed bases in either the minor, or major groove. The minor groove allows for smaller, often curved, molecules, to bind along the twisted DNA helix. In contrast, larger molecules, such as proteins, are instead more frequently found to bind in the major grove, in which their larger structural motives can be harbored. Lastly, a ligand can insert one or several parts of its structure in the hydrophobic space created between the stacked DNA base pairs, a process referred to as intercalation.

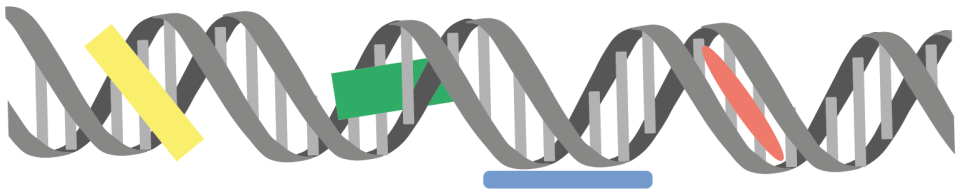

Figure 4: *Schematic illustration of the four different binding modes, major (yellow) and minor (red) groove binding, external binding (blue) and intercalation (green), to DNA.*

For the work presented in this thesis, two DNA binding molecules, the bis-intercalating cyanine dye YOYO-1 (YOYO), as well as the AT-selective grove binder netropsin, have been extensively used (Figure 5). When studying DNA with fluorescence microscopy (Section 3.1.2), the inherently non-fluorescent DNA needs to be stained with a dye in order to enable visualization. For this purpose, cyanine dyes, such as YOYO, display favorable photophysical properties including high binding constants, high emission quantum yields and low background fluorescence. Details on emission of light, including fluorescence, can be found in Section 3.1.1.

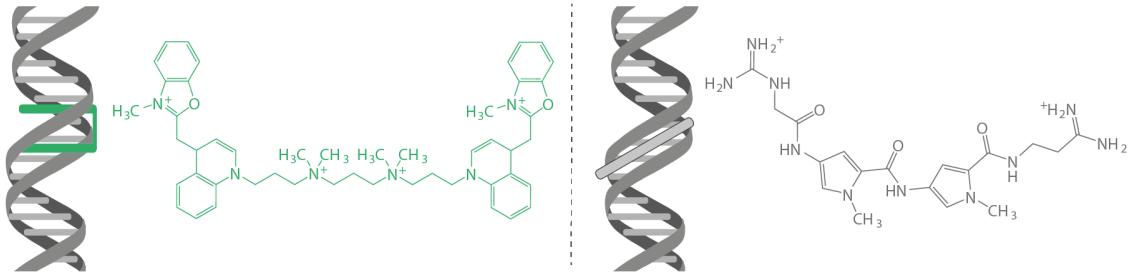

Figure 5: *Molecular structure and schematic representation of DNA binding molecules YOYO (left) and netropsin (right).*

YOYO binds to DNA by inserting its two aromatic ring structures in-between the base pairs, a process referred to as bis-intercalation (33, 34). When free in solution, YOYO is practically non-fluorescent, but once bound to DNA the rotation around the methane bridge is sterically hindered, increasing the emission more than a thousand-fold (33), making YOYO ideal for single molecule experiments. The maximum amount of YOYO bound to DNA, restricted by the nature of the binding mode, is approximately one YOYO molecule every four base pairs. External binding to the negatively charged DNA backbone is still possible, however at much lower binding affinities (34, 35). The binding of YOYO will also affect the structural properties of DNA. When inserting the two aromatic moieties between the DNA base pairs, YOYO will increase the effective contour length by 0.51 nm, as well as alter the helical twist, unwinding the DNA helix by approximately 24 degrees (36). Also, the positive charge (+4) of YOYO will reduce the overall negative charge of DNA.

Netropsin is a non-fluorescent, natural antibiotic, which binds selectively to AT base pairs displayed in the minor grove of the DNA helix. While the molecular structure of netropsin (Figure 5) allows it to form hydrogen bonds with adenine and thymine, giving rise to a strong and site specific binding, the amino group present in guanine will sterically hinder netropsin from forming hydrogen bonds to GC base pairs (37, 38). Hence, the strength of binding between netropsin and DNA will depend on the 5bp site on which netropsin binds, with 5'-AAAAA-3' allowing the strongest binding (39-41).

2.1.4 Enzymes for DNA Modification

As previously mentioned, proteins are long chains of amino acids linked via peptide bonds. Proteins are often referred to as the machinery of the cell, capable of performing a variety of functions. Different groups of proteins include transporter proteins, receptor proteins, structural proteins and enzymes. The latter function by accelerating chemical reactions, regulating a myriad of processes in a highly selective matter within a living cell. For instance, enzymes are essential in the process of replication, repair and modification of DNA.

One example of an enzyme involved in DNA modification is the Clustered Regularly Interspaced Short Palindromic Repeats (CRISPR) - associated protein-9 nuclease (Cas9) (42, 43), which has recently been developed into a gene editing tool capable of catalyzing highly sequence specific double stranded breaks, via the cleavage of the phosphodiester bonds in the DNA backbone (44, 45). The enzyme is involved in the adaptive immune system of bacteria and archaea (42, 46) and has found numerous scientific applications, including gene editing, targeting and regulation (47).

In order for the Cas9 enzyme to find the specific DNA sequence at which it will produce a double stranded break, it utilizes a RNA molecule displaying a 20 bp complementary sequence to the site of interest (Figure 6). This RNA molecule is called guide RNA (gRNA), and can be further dived in to two parts, termed tracrRNA and crRNA. The tracrRNA is responsible for the association to the Cas9 enzyme, while the crRNA provides the complementary 20 bp sequence to the targeted site on the DNA molecule. Hence, the sequence of the tracrRNA will stay the same, while the crRNA sequence can be selected depending on the site of interest on the DNA molecule. The only constraint when selecting the crRNA sequence is that it has to be followed by a three base sequence (NGG), termed protospacer adjacent motif (PAM), allowing nearly any existing gene to be targeted with high precision.

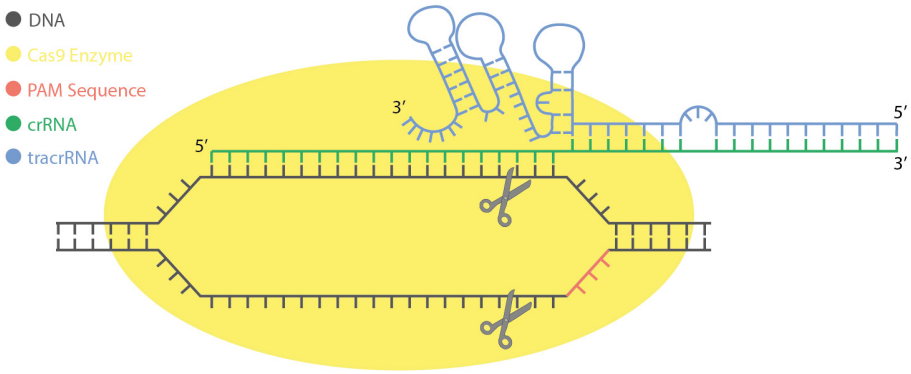

Figure 6: *Schematics of Cas9 binding and subsequent DNA cleavage aided by associated RNA molecules crRNA and tracrRNA. The double strand cleavage will take place approximately three nucleotides upstream of the protospacer adjacent motif (PAM) sequence.*

Forms of Cas9 that only selectively bind to DNA without producing a double strand break (48), as well as those only capable of producing a single strand break, have also been engineered. The first has been used in order to directly visualize sequence specific sites (49, 50), and the latter to induce double stranded breaks with higher precision (44, 51), or to mark the site of the single strand break by incorporating a fluorescent dye (52). Other enzymes capable of altering DNA, but with shorter recognition sites, are also readily available and have found several applications, for instance within the field of optical DNA mapping, further discussed in Section 2.4.

2.2 Bacteria and Their Plasmids

Bacteria are single cell organisms belonging to the family of prokaryotes, differing from human cells, eukaryotes, by not harboring membrane enclosed organelles. Only a few microns large, bacteria were one of the first life forms present on earth and can be found in a variety of different shapes and sizes (53). Bacteria reproduce by a process known as binary fission, where one mother cell divides to form two identical daughter cells.

Figure 7 depicts the main components of a bacterial cell. The cell wall provides structural strength and functions as a barrier that separates the bacterium from its surroundings. On the cell wall surface of some types of bacteria, there are small finger like extensions, known as pili, aiding in the exchange of genetic material between bacterial cells. The main

intracellular component, present in the cytoplasm of the bacteria, is the nucleoid, which besides small amounts of RNA and protein, mainly consists of chromosomal DNA. The cytoplasm also contains ribosomes for protein synthesis. Apart for the chromosomal DNA, responsible for maintaining essential cell functions, genetic information within bacteria can also be stored in plasmids.

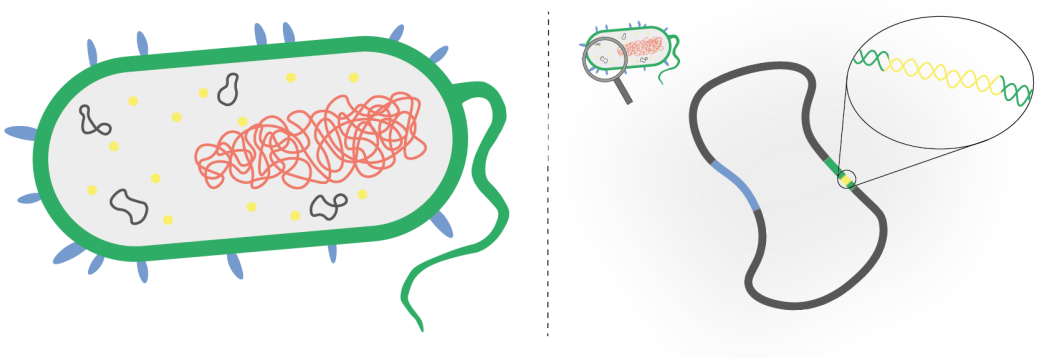

Figure 7: *Left: Simplified illustration of a bacterium and its major components. Cell wall and flagellum (green), pili (blue), nucleoid (red), ribosomes (yellow) and plasmids (gray). Right: Schematic illustration of a plasmid marked with a region encoding replication (green), including origin of replication (yellow), and a region encoding antibiotic resistance (blue).*

Termed by Lederberg in 1952 (54), plasmids are double stranded, circular DNA molecules, separate from the chromosome, capable of replicating autonomously. Figure 7 shows a schematic representation of a plasmid, including the origin of replication (ORI). The ORI, as indicated by the name, is the DNA sequence at which the replication of the plasmid starts. The minimal portion of the plasmid required for replication, the replicon, includes, beside the ORI, genes encoding proteins that assist in the replication process, as well as in plasmid maintenance. Different plasmids that share one or more elements of the replication mechanism cannot co-exist in the same cell, a phenomenon referred to as plasmid incompatibility (55). The copy number, *i.e.*, the number of copies of a specific plasmid within the cell, can range between a single to over a hundred (56), and the size spans between 1 kbp to over 1 mega base pair (Mbp).

Even though plasmids are not required for a bacterium to regulate and maintain its basic functions, they play a key role when a bacterium needs to adapt to a new environment, for instance when exposed to antibiotics (57). Plasmids are capable of horizontal gene transfer (details in Section 2.3.2), allowing them to spread between different bacterial strains and species. Moreover, plasmids are very dynamic, capable of amplifying beneficial genes, as well as deleting those that no longer have any desired function (58). Similarly, many plasmids possess the ability to insert external DNA into its sequence, hence acquiring new genetic material (8).

2.2.1 Current Methods for Plasmid Analysis

The dynamic nature of plasmids has made them central in the rapid spread of antibiotic resistance (Section 2.3), but at the same time hard to study. However, there are tools available for characterizing plasmids, allowing information about size, type and sequence to be extracted. As a standard method for plasmid sizing, S1-coupled pulsed field gel electrophoresis (S1/PFGE) is used (9). After linearization via S1 nuclease (59), the plasmids are separated by applying an alternating (pulsed) electric field over an agarose gel, in which the plasmids migrate due to their negatively charged DNA backbone. Since smaller DNA molecules will travel faster through the pores of the gel, a non-linear separation based on size is obtained. Staining the DNA with a fluorescent dye enables visualization of the dominating plasmid bands on the gel. By adding DNA molecules of pre-known size to the same experiment as reference, the size of the plasmids can be determined.

There are several methods for plasmid characterization that are based on the polymerase chain reaction (PCR) (60). The general idea is to find out if a particular sequence, defined in advance, is present on the DNA molecule of interest, in this case a plasmid. The PCR reaction can be divided into three main steps: denaturation, annealing and elongation. After heating the DNA, causing the DNA to denature into two separate strands, pre-designed, short base pair sequences, complementary to the sequence of interest (primers) are added to the reaction. Once the primers have annealed with the single stranded DNA, the DNA is elongated by further addition of nucleotides and a DNA polymerase. Provided that the sequence is present, there is a two-fold increase of the targeted DNA sequence each time the cycle is repeated. The targeted sequence is detected by performing gel electrophoresis on the PCR product, or by using quantitative real time PCR (qPCR), utilizing fluorescence for instant read out during the experiment (61).

Plasmid based replicon typing (PBRT) utilizes PCR in order to group plasmids based on their replication mechanism (10, 62). In the otherwise very dynamic plasmids, the replicon is a highly conserved region, making it an ideal target for plasmid classification. As mentioned in Section 2.2, two plasmids that share one or more parts of their replication mechanism cannot propagate in the same bacterial cell, they are said to be incompatible. Designing primers complementary to different regions found in the replicon thus allows plasmids to be divided into different groups based on their incompatibility, referred to as Inc groups. It should be noted that one plasmid can have multiple replicons, hence the number of different plasmids in a sample is not necessarily directly related to the number of replicons found.

Additionally, plasmid multi locus sequence typing (pMLST) can be used to classify plasmids further (10, 63). Using pMLST the most common Inc groups are divided into different subgroups. Here primers are designed to target additional sites along the plasmid, including genes involved in plasmid maintenance and transfer, resulting in a more precise characterization. Furthermore, PCR can be used to target a specific gene of interest, for example a gene known to encode antibiotic resistance. In order to ensure that the gene is present, multiple primers are used, targeting different positions along the same gene.

Finally, there is the option of DNA sequencing for plasmid characterization. There are many different approaches for sequencing of DNA molecules (11, 64, 65), but most of them follow the same basic principles. First, the DNA is fragmented into smaller pieces, normally from ten up to a couple of hundreds of bp in size (66). The fragments are then amplified using PCR, and later sequenced individually. In order to obtain the full DNA sequence, these fragments, termed reads, need to be assembled. By generating many copies of the DNA sequence of interest, and relying on the fragmentation process to be random, the idea is that there will be an overlap between different reads, making them possible to puzzle back together.

If the correct sequence can be assembled, DNA sequencing provides information about a plasmid down to the base pair level, allowing accurate size estimation as well as information about which genes the plasmid harbors. For reliable results, a general guideline is that each nucleotide should be sequenced a number of times, referred to as coverage, requiring multiple copies of identical plasmids in order to assemble the sequence with high accuracy. New technologies (67), relying on high quality samples, have made it possible to generate longer read lengths, aiding in the process of assembling

intact plasmids (68), a process which is far from trivial due to the dynamic nature of plasmids.

2.3 Antibiotic Resistance

"The thoughtless person playing with penicillin treatment is morally responsible for the death of the man who succumbs to infection with the penicillin-resistant organism"

– Sir Alexander Fleming, 1945

Antibiotics are antimicrobial drugs commonly used to treat, and prevent, bacterial infections. Starting with the discovery of penicillin by Fleming almost a century ago (1, 2), antibiotics have become a corner stone of modern health care. However, severe overuse, both for humans as well as for livestock, in combination with no new major antibiotic discoveries the past decades, has led to a radical increase in the degree of resistant bacteria worldwide (3, 4). If the development continues, the prognosis is one person dying every third second due to non-treatable bacterial infections by 2050, even outcompeting the death rates of cancer globally (3).

To reverse the trend, there is a need to target the problem on multiple fronts (3). New antimicrobial drugs need to be developed, either via compounds similar to the traditional antibiotics used today, or by novel strategies including phage therapy, antibodies and antimicrobial peptides (69). The use of existing antibiotics needs to be drastically decreased via actions such as increased public awareness, improved hygiene and sanitary routines, as well as new policies for the use of antibiotics in agriculture and the environment. Finally, there is an urgent need for tools capable of rapid diagnostics of resistant bacteria. At present, diagnostics of bacterial infections are based on empirical observations as well as culture-based approaches (Figure 8). Diagnostics via bacterial cultivation in presence of different types of antibiotics is an inherently time consuming process, spanning over more than 36 hours, and is further hampered by pathogenic bacteria frequently failing to grow in samples from patients with clinical signs of infection (5). Rapid diagnostics would not only be beneficial for a patient with a severe bacterial infection, but also allow to use existing antibiotics more efficiently, sparing the use of last resort antibiotics to when they are truly needed.

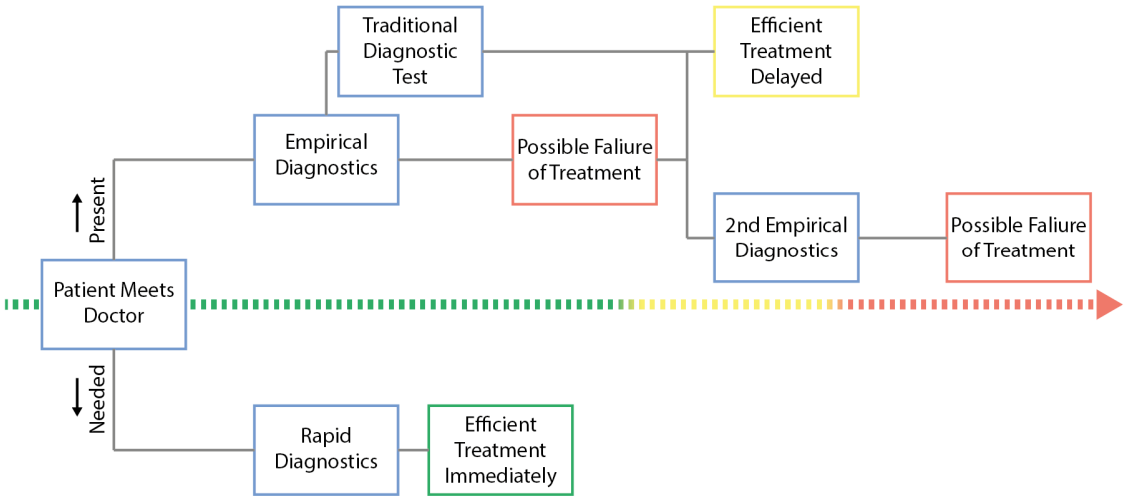

Figure 8: *Schematic flowchart of present and desired paths for bacterial diagnostics.*

As discussed above, one of the main reasons for the rapid spread of antibiotic resistance is bacterial plasmids (8, 12, 70). The ability of a plasmid to transfer between different strains and species via a process known as conjugation, a type of horizontal gene transfer (Section 2.3.2), as well as their very dynamic nature, have made plasmids highly advantageous for acquiring antibiotic resistance genes. Recently, plasmid mediated resistance has been reported for last resort antibiotics, such as polymyxins (71) and carbapenemes (70), emphasizing the need of efficient methods to monitor and study plasmids.

2.3.1 Mechanisms of Defense

Antibiotic resistance can be obtained through spontaneous mutations, or acquired via horizontal gene transfer. The outcome of treating a bacteria with an antibiotic which it has acquired a resistance gene against will be the same, however the resistance mechanism encoded by the gene can differ. Four main defense mechanisms of bacteria to antibiotics are shown in Figure 9 (56, 72, 73).

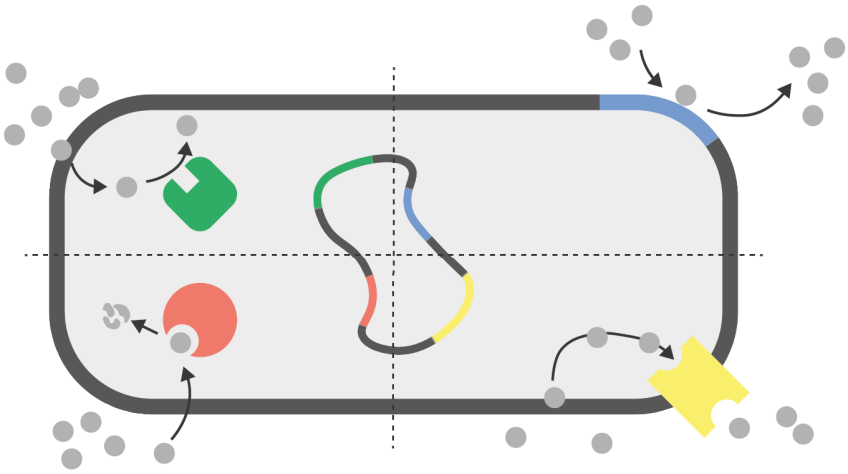

Figure 9: *Illustration showing four main bacterial defense mechanisms against antibiotics. Circular path in the center of the image represents a plasmid encoding resistance via: modification of drug target (green), altered cell wall composition (blue), utilization of cell wall attached protein pumps (yellow) and enzymatic degradation (red).*

Each antibiotic is designed to specifically target a part of an essential process for long term bacterial survival. The antibiotic usually targets a structural component within the bacterial cell, such as a protein, altering its function, and hence altering the process the protein is involved in. By changing the motif the antibiotic is designed to bind, but which does not change the function of the bacterial component itself, the effect of the antibiotic is neutralized. Other approaches the bacteria can use as defense include alteration of the cell wall, hindering the antibiotic from entering, as well as utilizing cell wall proteins capable of removing the antibiotic ones it has entered the cell.

Finally, the bacteria can also produce enzymes capable of altering, or degrading, the antibiotic. One example of such enzymes are β-lactamases, with the ability to degrade antibiotics belonging to the group of β-lactams, including penicillin. β-lactam antibiotics interfere with the cell wall synthesis of the bacteria, both by resource depletion and by inhibiting the synthesis process (74). However, if the β-lactamase enzyme cleaves the β-lactam ring of the antibiotic, the activity is lost and the bacteria is left unharmed.

2.3.2 Gene Transfer

There are two main modes of how resistance genes can be transferred, vertically and horizontally (73). Vertical transfer is when a spontaneous mutation occurs, rendering a progeny slightly different than its ancestor. Far from all mutations will provide a selective advantage, but by chance a minor fraction of them will allow the bacteria to increase their fitness compared to their previous generation. In contrast, horizontal gene transfer is a process in which foreign genetic material is acquired by a bacterium. There are three main mechanisms of horizontal gene transfer: transformation, transduction and conjugation (73, 75). Transformation is a process in which foreign material is taken up by a bacterium from the surrounding environment. In transduction, DNA is transferred via bacteriophages, which are bacterial viruses, inserting their DNA into the bacterial genome. Lastly, entire plasmids can be transferred from one bacterium to another in a process known as conjugation (Figure 10) (57, 73, 75, 76).

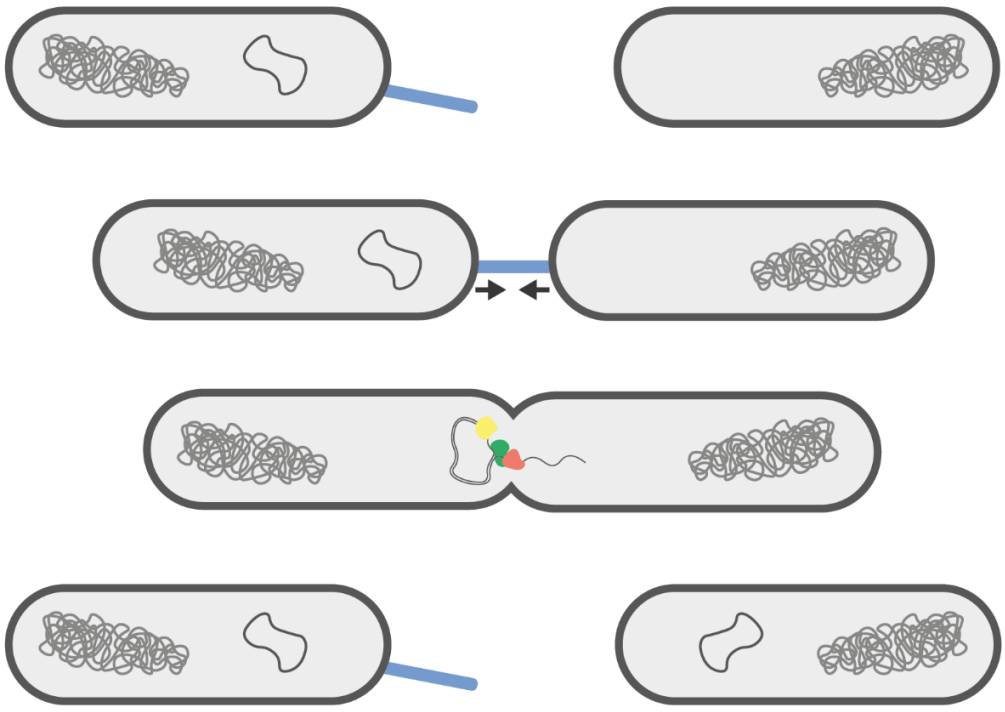

Figure 10: *The process of conjugation, transfer of a plasmid from a donor cell to a recipient. Image depicts pili (blue), responsible for cell to cell contact, and key enzymes, DNA-polymerase (yellow), transferase (red) and relaxase (green), involved in the replication and transfer mechanism.*

Conjugation is a contact dependent process, aided by a pilus on the donor bacterium, which attaches to the cell wall of the recipient. The DNA polymerase replicates the plasmid in order for both the donor and recipient to end up with a copy. Additionally, two protein complexes, transferasomes and relaxomes, assist in the simultaneous transfer mechanism (76). Due to the number of genes required for a plasmid to be transferred, conjugative plasmids tend to be larger than 30 kbp (7). Since the entire plasmid is transferred, a plasmid harboring resistance genes against a variety of antibiotics, can make a fully susceptible bacterium multi resistant in one step.

2.4 Optical DNA Mapping

Optical DNA mapping is based on visualizing long range sequence information on individual DNA molecules at the kbp level. The DNA is labeled in a sequence specific manner, stretched, and finally imaged, generally using a fluorescence microscope. Advantages of using optical mapping to study DNA include remarkable read lengths, spanning up to 1 Mbp, as well as extracting information on single molecule fluctuations, avoiding averaging. Below follows a brief overview of the progress which has been made within the filed, including strategies for labeling and stretching of DNA. For a more detailed description the reader is referred to the following reviews (15, 16, 77-81).

Since the pioneering work by Schwartz et al. (14), utilizing restriction enzymes to cut the DNA molecules at specific sites, and subsequently visualizing the length of the different fragments in an agarose gel, the field of optical DNA mapping has advanced significantly. Different approaches for stretching and labeling have been developed. Main techniques for extending DNA include molecular combing (82, 83), were DNA is stretched on modified glass surfaces, as well as nanofluidic devices (84), in which DNA is extended by confinement to nanofluidic channels. Labeling strategies can be divided into two main categories, enzyme based labeling, and affinity based labeling, illustrated in Figure 11.

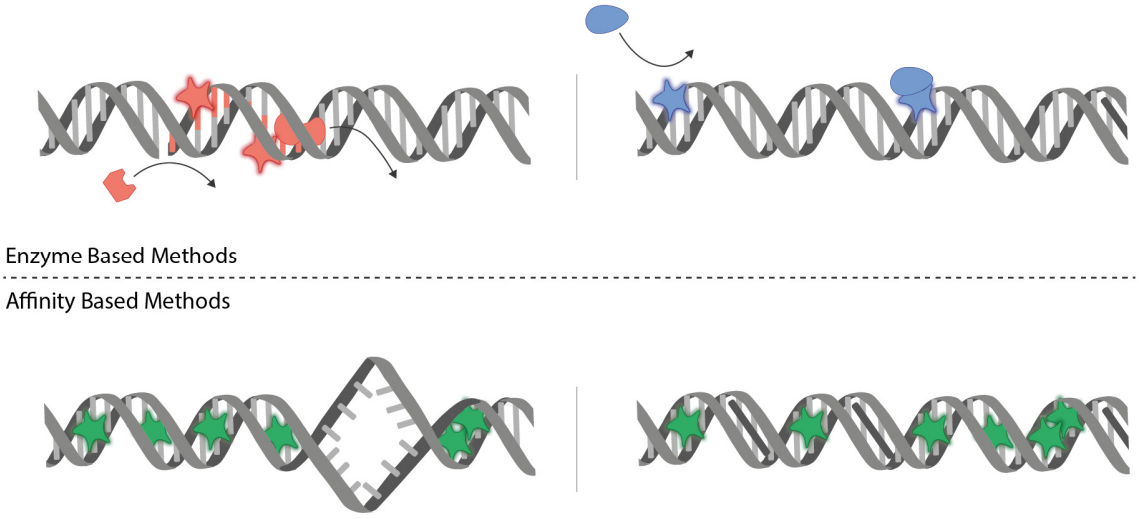

Figure 11: *Schematic illustration of the most common labeling strategies for optical mapping of DNA. Top Left: Nick labeling, where a nicking enzyme creates a single strand break at its recognition site, typically 4-7bp long. A DNA polymerase later removes old, and incorporates new fluorescently labeled, nucleotides, in order to visualize the site. Top Right: Methyltransferase based labeling, where a fluorescently labeled methyl group is transferred to the DNA at a specific recognition site. Bottom Left: Denaturation mapping, utilizing the lower melting temperature of AT base pairs compared to GC base pairs. Staining the DNA with the fluorescent dye YOYO, which prefers dsDNA over ssDNA, and carefully increasing the temperature, will result in dissociation of YOYO subsequent to the local melting of AT base pairs. Bottom Right: Labeling via competitive binding between the AT specific, non-fluorescent, molecule netropsin and YOYO. Netropsin will bind to AT sites, blocking these from YOYO, creating an emission profile along the DNA where AT-rich regions are dark, and GC-rich regions bright.*

Introduced by Jo et al. (85), nick labeling is based on incorporating fluorescently labeled nucleotides at sequence specific sites (Figure 11). First, a nicking enzyme generates a single stranded break, referred to as nick, at its recognition site, typically 4-7 bp long. Next, a DNA polymerase is used to remove, and subsequently incorporate, new fluorescently labeled nucleotides along the strand. In order to determine the start and end of each molecule, YOYO is used to stain the full contour of the DNA molecule. Depending on the sensitivity of the application, the DNA can be repaired from any existing nicks previous to the assay, avoiding false positives, and excess nucleotides removed afterwards, in order to decrease the background fluorescence.

Das et al. later extended the nick labeling assay, introducing a nick-flap labeling scheme (86). By using a DNA polymerase lacking exonuclease activity, the nucleotides following the nicking site are displaced rather then removed, leaving a single stranded flap of DNA. This allows for dual labeling, including the nicking site, as well as the flap, using a complementary, labeled, oligonucleotide. Moreover, Hastie et al. used a dual labeling approach, using two nicking enzymes with different recognition sites (87). Performing the reactions consecutively, with an intermediate purification step, allowed the use of differently labeled nucleotides and thus a dual color readout. In order to address the limited specificity of the available nicking enzymes, McCaffery et al. further extended the nick labeling assay using a CRISPR/Cas9 based approach, enabling the use of a highly adaptable 23 bp long recognition site (52). Nick labeling, in combination with nanochannel based DNA extension, has been commercialized via BioNanoGenomics, allowing for a range of applications, including de novo assembly of complex genomes where the optical maps are used as templates (88-99).

Similar to nick labeling, methyltransferases can be used in order to label DNA in a sequence specific manner (100, 101). The enzyme recognizes a site, typically 4 bp, and transfers a fluorescently labeled methyl group to the DNA (Figure 11). Vranken et al. used this approach to achieve optical maps with nanometer resolution (102). Methyltransferase labeling has also been used to generate densely labeled DNA, termed amplitude modulation profiles, taking advantage of the short recognition site of the enzyme (103). Additional to nick and methyltransferase based labeling, there is also the possibility to extract information beyond the DNA sequence. Applications include epigenetic marks in the form of methylations (104), and hydroxymethylations (105, 106), as well as histone modifications (107). Furthermore, DNA damage sites have been successfully fluorescently labeled and visualized after stretching the DNA molecules on a glass surface (108).

Denaturation mapping, developed by Reisner et al. (109), utilizes the lower melting temperature of AT base pairs, which are connected by two hydrogen bonds, compared to GC base pairs, which have three hydrogen bonds. By staining the entire DNA contour with the fluorescent dye YOYO and carefully increasing the temperature, AT base pairs will melt, causing YOYO, which prefers dsDNA over ssDNA, to dissociate. This will create an emission intensity profile along the extension of the DNA, where AT-rich regions will be dark, and GC-rich regions bright. The DNA can be heated either on chip (109, 110), or before sample loading (111).

Recently, a complementary approach for labeling DNA, based on competitive binding, has been established (112, 113). When simultaneously adding the AT specific, non-fluorescent, molecule netropsin, and the fluorescent dye YOYO, the molecules will compete for the binding sites on the DNA. If added in a correct ratio, netropsin will block the AT-sites, preventing YOYO to bind, rendering an emission intensity profile along the DNA, where AT-rich regions will appear dark, and GC-rich regions bright. With the competitive binding assay, which has been used throughout the work presented in the Thesis, there is no need for repair of the DNA before labeling, performing additional purification steps, or achieving precise temperature control.

3 Methodology and Fundamental Concepts

In this section, the methods used in the Thesis are described, as well as some related fundamental concepts. First, a brief theory on the emission of light is provided that is later coupled to a description of fluorescence microscopy. Background is also given on the concept of DNA in nanofluidics, including chip design and experimental setup.

3.1 Emission of Light

The interaction between light (photons) and matter will depend on the electronic configuration of the irradiated molecules in the sample. The energy of the photons, described by their wavelength, can be absorbed by a molecule via the excitation of an electron. For excitation to occur, the energy of the photon needs to match the energy gap between an excited state of the molecule (S_n) and its ground state (S_0). A Jablonski diagram, shown in Figure 12, illustrates the different excitation and de-excitation processes occurring when a molecule interacts with light.

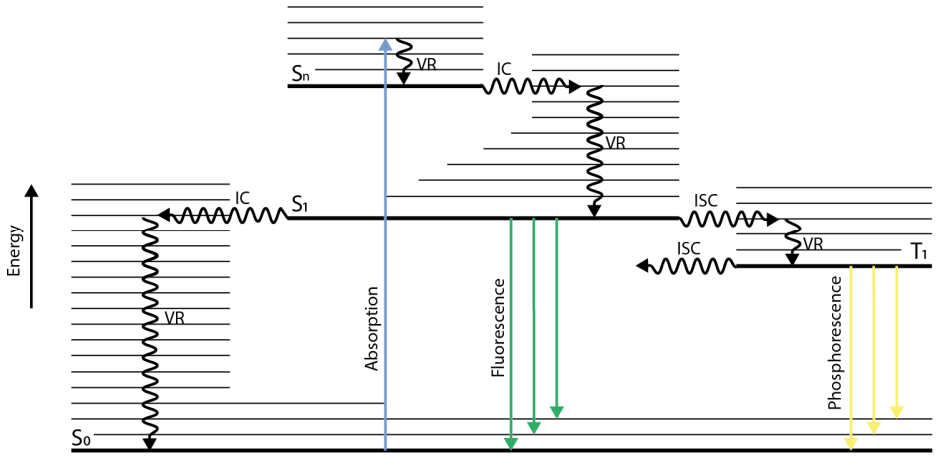

Figure 12: *A Jablonski diagram showing absorption and excited state deactivation pathways of a molecule. Singlet (S_0, S_1 and S_n) and triplet (T_1) states are shown with bold horizontal lines, with corresponding vibrionic states as non-bold horizontal lines. Radiative processes, including absorption (blue), fluorescence (green) and phosphorescence (yellow), are displayed as straight vertical arrows. The non-radiative processes internal conversion (IC), inter system crossing (ISC) and vibrational relaxation (VR) are shown as undulating arrows.*

When a photon is absorbed by a molecule, the absorbed energy will lead to a re-configuration of the electrons within the molecule, resulting in what is referred to as an excited state. The excited states, both singlet (S_n), with paired electrons, and triplet (T_n), with unpaired electrons, are numbered in a consecutive order based on their energy gap relative to the ground state. Each electronic state is also associated with a number of vibrational states, which are typically closer in energy.

Following excitation to S_n, the molecule will typically undergo rapid relaxation to the lowest vibrational energy of the first excited state (S_1), via a combination of vibrational relaxation and internal conversion. Hence, excited state processes can be approximated to only occur from the lowest vibrational state of S_1, a phenomena referred to as Kasha's rule (114). Once in S_1, the molecule can return to the ground state via three main routes: non-radiative relaxation, emission from the first excited singlet state (S_1) and decay through the first excited triplet state (T_1). For non-radiative relaxation, the molecule undergoes internal conversion from S_1 to S_0, followed by vibrational relaxation (Figure 12), dissipating the excess energy to the surrounding environment. Deactivation via

radiative relaxation from in S_1 to S_0 is termed fluorescence, and results in an emitted photon. Deactivation via T_1 involves inter system crossing, where the molecule undergoes a spin-forbidden transition, rendering a state with unpaired electrons. From T_1 the molecule can either return to its ground state via emitting a photon, known as phosphorescence, of by relaxing non-radiatively (Figure 12). Which deactivation pathway that dominates will depend on the structure of the molecule, as well as the surrounding environment.

The wavelength of an emitted photon is typically longer than the wavelength used for excitation. For fluorescence, the difference in wavelength is referred to as the Stokes shift (115). The Stokes shift can be explained by the rapid relaxation from S_n to S_1, the tendency of a molecule to return to an excited vibrational state of S_0 upon emission, as well as excited-state reactions and solvent relaxation effects. The efficiency of the fluorescence process is described in terms of the quantum yield, which is a measure of how many times a specific event, such as fluorescence, occurs per photon absorbed by the molecule. Moreover, the amount of emitted photons will depend on the ability of a molecule to absorb light, which is governed by the molar absorptivity (ε) at each wavelength.

The preferred properties of a fluorescent molecule, a so called fluorophore, vary depending on application. In general, a high quantum yield, in combination with a high molar absorptivity is desirable, providing a bright fluorophore. Furthermore, a distinct Stokes shift allows separation of excitation and emission more efficiently. For instance, the fluorophore YOYO, used in the work presented in the Thesis, has a quantum yield of 0.52, molar absorptivity of 10^5 $M^{-1}cm^{-1}$ at 491 nm and an emission maximum at 509 nm when bound to dsDNA (33).

3.2 Fluorescence Microscopy

Fluorescence microscopy has been extensively used throughout the work presented in the Thesis. In contrast to other optical microscopy techniques, relying on reflection and absorption, fluorescence microscopy utilizes emission to visualize a substrate. For inherently non-fluorescent molecules, such as DNA, a fluorophore can be used to enable visualization. The principle setup of an inverted fluorescence microscope is shown in Figure 13.

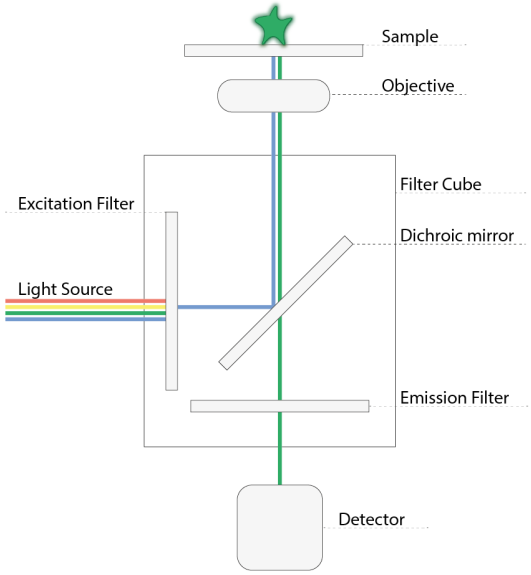

Figure 13: *Schematic image depicting the main components of an inverted fluorescence microscope.*

The main components of a fluorescence microscope include: an excitation light source, two filters, one for excitation and one for emission, an objective to focus the light onto the sample, as well as a detector recording the emitted photons. The light source can either be monochromatic, or contain a broad spectrum of wavelengths. The excitation and emission filters are usually combined with a dichroic mirror, possessing the ability to reflect excitation light and transmit emitted light. The three components make up a so called filter cube, which can be changed in order to match the maximum excitation and emission wavelengths of the selected fluorophore.

In short, light is sent through the excitation filter in order to match the excitation wavelength of the fluorophore of interest. The transmitted light is reflected on a dichroic mirror and focused through an objective before reaching the sample. The back-scattered fluorescence emission is then collected through the same objective and transmitted through the dichroic mirror and emission filter before reaching the detector. Detection is typically enabled via a sensitive camera, such as a complementary metal oxide semiconductor (CMOS) or an electron multiplying charged coupled device (EMCCD).

3.3 DNA in Nanofluidic Devices

There are different approaches for stretching individual DNA molecules, including the use of magnetic or optical tweezers, flow, molecular combing, and nanofluidic channels (116). For optical DNA mapping, stretching DNA on modified glass surfaces, known as molecular combing, or extending DNA in nanofluidic channels, are the most common approaches. While molecular combing offers a rapid overview of many molecules, in combination with being readily accessible, uniform stretching is not guaranteed. When stretching DNA by confinement in nanofluidic channels, a position X% into the contour of the DNA will correspond to X% into the sequence, thus allowing sequence specific information to be extracted with high precision. Nanofluidic devices also offer the possibility of automation, allowing for high throughput applications.

Utilizing the advances made in the field of microelectronics, techniques for fabrication of nanofluidics chips have been established (77). Generally the nanofluidic chips are fabricated from oxidized silicon, also known as silica, due to its high availability and favorable properties. The low surface roughness and negative charge of the silica prevents DNA molecules from adhering to the channel walls. Also, the hydrophilic nature of the material promotes wetting once DNA and buffer are added to the chip. The design of the nanofluidic chip used for the work presented in the Thesis is shown in Figure 14.

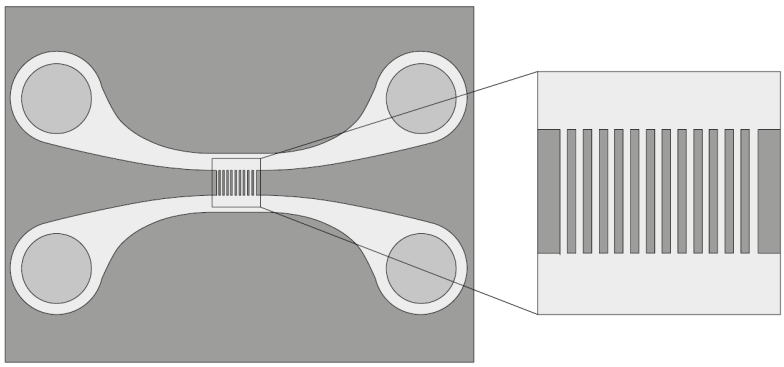

Figure 14: *Schematics of a nanofluidic chip showing four circular loading wells, connected two and two by microchannels, which in turn are spanned by a set of nanochannels (zoom).*

The nanofluidic chip used for the work presented in the Thesis, and shown schematically in Figure 14, has four wells for sample loading, connected two and two via microchannels. The microchannels are in turn spanned by a set of nanochannels with dimensions of 100 x 150 nm (width x height) and a length of 500 μm. The nanofluidic chips are made from a 500 μm thick silicon wafer using standard clean room procedures including: thermal oxidation, photolithography, E-beam lithography, reactive ion etching (RIE) and fusion bonding. In order to allow visualization of the DNA inside the nanofluidic channels, the chip is sealed with a transparent Pyrex glass lid.

Over the years, various designs of nanofluidic chips have been demonstrated, tailor made for their specific applications. Approaches include, tapered nanochannels allowing to measure extension of a DNA molecule at different degrees of confinement (117), entropic gradients lowering the entropy barrier by pre-stretching the DNA prior to entering the nanochannel (90), as well as meandering channels in order to visualize Mbp sized DNA molecules in one single frame (118). Moreover, post processing procedures, such as lipid passivation (119), are available and can prevent proteins and other biological molecules from adhering to the channel walls. For more details on the fabrication process of nanofluidic chips the reader is referred to the following reviews (23, 77, 120).

In order to visualize and image the DNA when confined in the nanofluidic channels an experimental set-up based on fluorescence microscopy, as schematically shown in Figure 15, was used for the work presented in the Thesis. The chip is mounted onto a chip holder which in turn is placed on the microscope. Besides functioning as a support for placing the chip in contact with the objective of the microscope, the chip holder provides access to the loading wells of the chip, allowing to add the sample, as well as to move the DNA inside the chip via the use of pressure driven N_2 flow. A 100x oil immersion objective with numerical aperture of 1.46 in combination with an EMCCD camera was used for imaging.

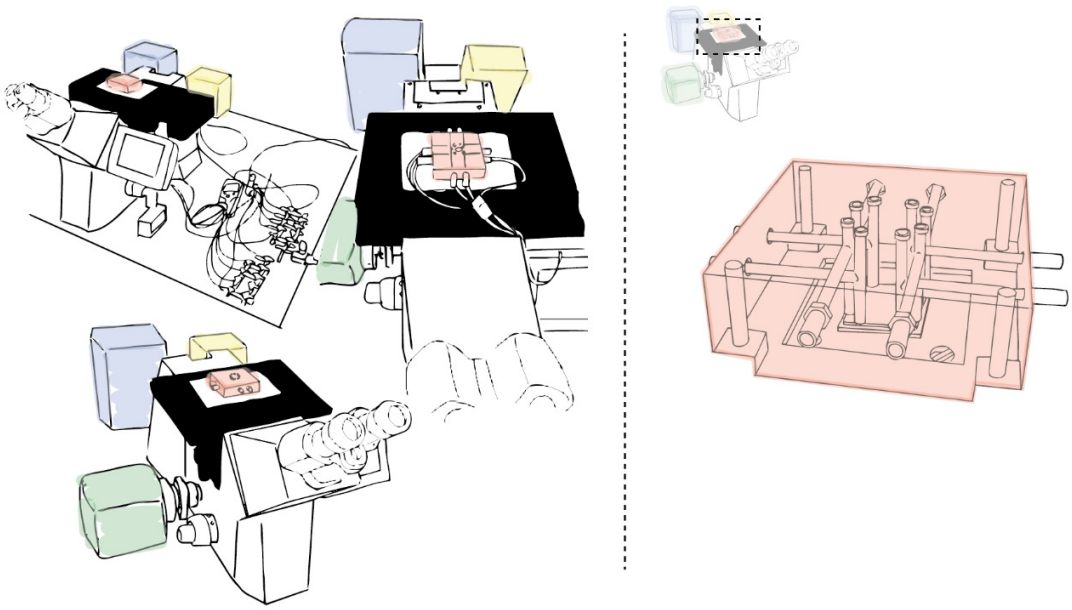

Figure 15: *Left: Illustration of the experimental setup used for the research presented in the Thesis. The EMCCD camera is shown in green, the fluorescence lamp in blue, the bright field lamp in yellow and the chip holder in red. Right: Schematics of the chip holder with the nanofluidic chip mounted underneath (bottom), inlets for sample loading (top) and connections for applying pressure to specific loading wells (side).*

4 Summary of Results

In this chapter, the work on which the Thesis is based will be discussed and summarized. An overview of the results presented in the appended papers is provided, starting with a brief introduction to the developed assay, followed by some general information on the experimental procedure and subsequent data analysis. For further details on the presented research, the reader is referred to the appended papers.

4.1 Assay Development

As previously discussed, one of the main reasons for the rapid spread of antibiotic resistance is horizontal gene transfer of mobile genetic elements, such as plasmids. Therefore, tools allowing the epidemiology and evolution of plasmids to be studied are of great interest. Moreover, there is an urgent need for rapid POC diagnostics in order to enable more efficient treatment of serious bacterial infections, as well as to spare last resort antibiotics to when really needed.

To meet this need, an assay was developed for rapid characterization of intact plasmid molecules, based on the previously established competitive binding scheme of YOYO and netropsin (112, 113). The advantage of optical DNA mapping compared to existing strategies for plasmid analysis include the low amount of sample required, as well as obtaining long range sequence information from the intact plasmid sequence. An overview of the current version of the assay, developed in **Paper I-III**, can be seen in Figure 16.

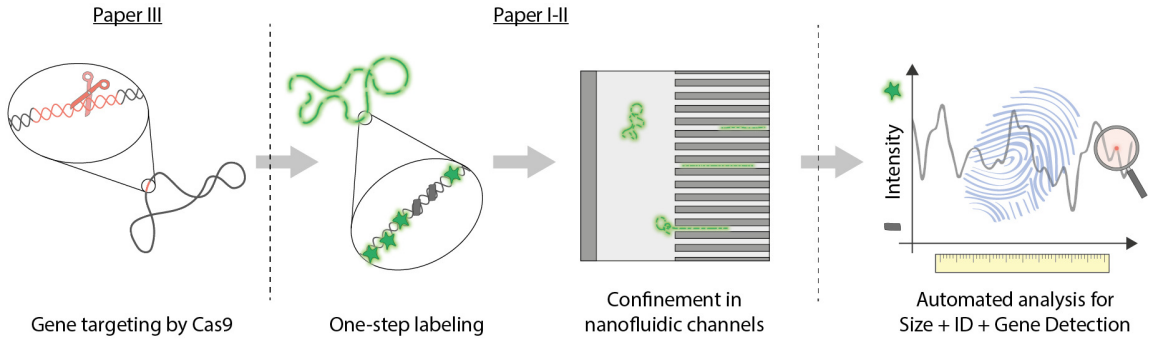

Figure 16: *Overview of the assay developed in Paper I-III. In the first step the plasmid is cut by Cas9 (red scissors) at the site of the targeted gene. In the second step, YOYO (green star) and netropsin (gray rectangle) are added to the sample, creating an emission intensity profile along the DNA based on the underlying sequence. In the third step, nanofluidic channels are used to stretch the DNA, allowing the emission profile along the contour of the DNA to be visualized using fluorescence microscopy. Following the data analysis, the size of all plasmids, a corresponding "fingerprint" for identification and tracking, as well as information on the presence or absence of a specific gene is acquired.*

The work presented in **Paper I** (details in Section 4.2) allowed us to identify plasmids encoding genes for antibiotic resistance by comparing to a database containing all known plasmid sequences. In **Paper II** (details in Section 4.3) we were able to identify and trace plasmids in clinical samples from a nosocomial outbreak at a neonatal ward at Sahlgrenska University Hospital. Moreover, using an approach based on CRISPR/Cas9, we demonstrated in **Paper III** (details in Section 4.4) how the assay could be expanded to simultaneously detect (resistance) genes on individual plasmids.

In short, the assay, as illustrated in Figure 16, shows how the resistance gene is selectively cut by the Cas9 enzyme, before subsequent staining with YOYO and netropsin. The DNA is later stretched in nanofluidic channels, allowing for visualization using fluorescence microscopy. Finally, analysis of the data reveals the number of plasmids in the sample, their corresponding size and sequence specific intensity profiles, as well as the presence or absence of a targeted gene.

4.1.1 Experimental Procedure

In this section, some general considerations of the experimental procedures for the three presented papers are provided, beginning with the plasmid samples that have been provided by our collaborators at Uppsala University and Sahlgrenska University Hospital. Following cultivation of clinically relevant bacterial isolates, the plasmids were extracted using standard commercialized kits. First the DNA was separated from the additional components of the bacterial cell, followed by separation of the circular plasmids from the chromosomal DNA.

The plasmid samples were stained using an approach based on competitive binding between YOYO and netropsin, as described in Section 2.4 (112, 113). In short, the non-fluorescent, AT-specific, molecule netropsin, competes with the fluorescent dye YOYO for the AT-rich regions, resulting in an overall lower emission from AT-rich regions than from GC-rich regions along the extension of the DNA molecule (Figure 17). In order to compensate for the lower overall binding affinity to DNA, netropsin was generally added at a ratio of 150:1 with respect to YOYO. The obtained intensity profile serves as a "fingerprint" for the DNA molecule, based on the underlying sequence (Figure 17).

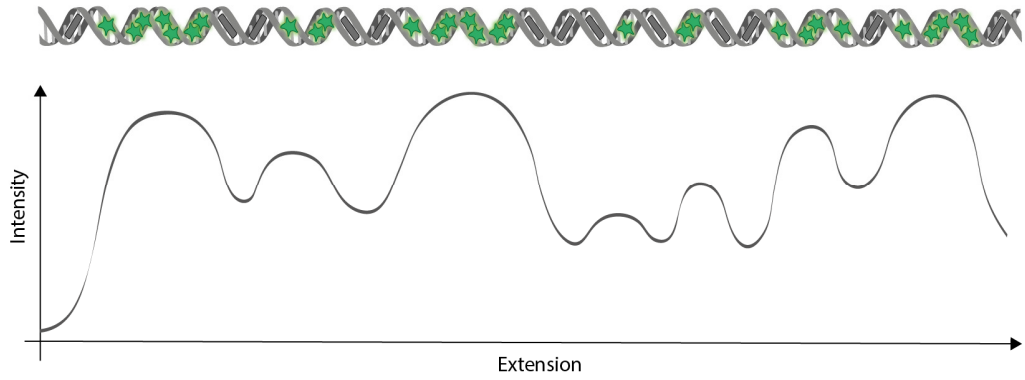

Figure 17: *Schematic illustration of the emission intensity profile created by the competitive binding of YOYO (green star) and netropsin (gray rectangle) to DNA, serving as a "fingerprint" of the underlying DNA sequence.*

In addition to YOYO and netropsin, lambda DNA was added to the plasmid sample as an internal size reference. The size of the linear lambda DNA molecule (48 502 bp) is previously known, allowing a conversion factor to be calculated, relating the extension in pixels to the number of bp of an observed plasmid. Since lambda DNA was added to each plasmid sample, it was possible to compensate for minor deviations in the experimental conditions, including factors such as ionic strength and nanochannel dimensions.

In order to facilitate rapid equilibration, the DNA was stained with YOYO and netropsin at high ionic strength and heated to 50 °C (121). The high ionic strength shields the negatively charged DNA backbone, increasing the rate of dissociation of the positively charged YOYO molecule, facilitating rapid rearrangement along the DNA. However, as previously discussed in Section 2.1.2, a high ionic strength will decrease the degree of extension of DNA when confined to nanofluidic channels (77). Therefore, subsequent to the labeling, the sample was diluted approximately 100 times with ultrapure water, providing a solution of much lower ionic strength.

When exposing YOYO to light in the presence of oxygen, oxygen radicals will be formed, capable of producing single strand breaks on the DNA (122), a process referred to as photo-nicking. If two single strand breaks occur close enough on each of the DNA strands, the dsDNA will break. In order to reduce the amount of photo-nicking, the oxygen radical scavenger β-mercaptoethanol (BME) was added to the solution.

As briefly mentioned in Section 3.3, an epi fluorescence microscope, allowing access to the chip from below, with the objective facing the glass lid of the chip, was used for the work presented in the Thesis. The use of a 100x oil immersion objective with a numerical aperture of 1.46, in combination with an EMCCD camera, sets a resolution limit on the optical DNA maps of typically 1 kbp. The resolution is limited by the dimensions of the nanochannels, governing the degree of extension, as well as the fundamental resolution limit of optical microscopy. An image of plasmids inside the micro and nanochannels of the chip, visualized with fluorescence microscopy, is shown in Figure 18.

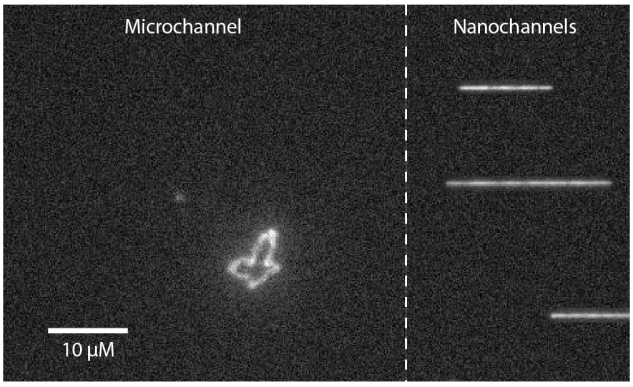

Figure 18: *Fluorescence microscopy image of one plasmid inside the larger microchannel (50 µm x 850 nm), and three plasmids confined inside the narrower nanochannels (100 nm x 150 nm).*

In order to control the movement of the DNA inside the nanofluidic chip, a N_2 flow system was used. The rationale for using N_2 in the flow system, rather than air, was to reduce the overall concentration of O_2 in the sample, preventing extensive photo-nicking of the DNA. By connecting one switch to each loading well, DNA can be flushed inside the microchannel by applying pressure to one of the wells, and subsequently forced into the nanochannels, by applying pressure to both sides of the microchannel (Figure 14, 15 and 18). Once confined, a series of typically 200 images, with an exposure time of 100 ms, was taken of the extended DNA molecules.

4.1.2 Data Analysis

The data analysis tools used for the work presented in the Thesis have been developed in collaboration with Tobias Ambjörnsson's group at Lund University. The Matlab based software has been continuously improved throughout the presented work, adding new features for each appended paper. An overview of the data analysis workflow can be seen in Figure 19.

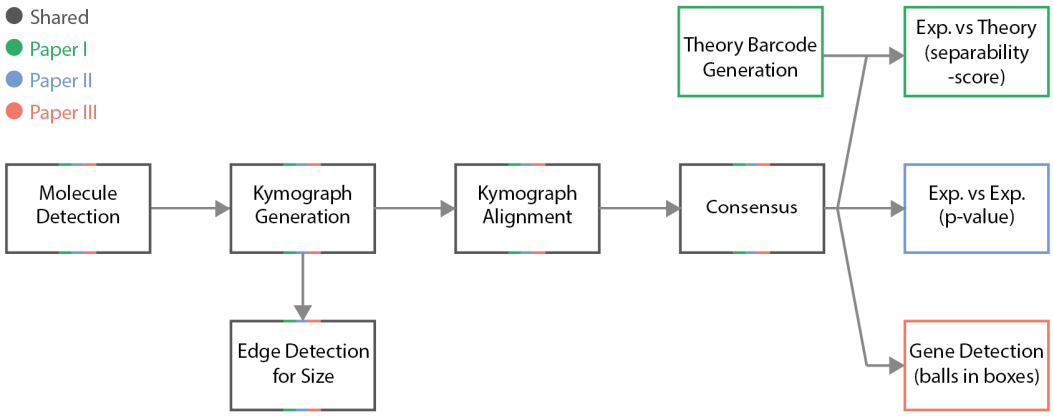

Figure 19: *Work flow over the data analysis steps used in the work presented in the Thesis.*

Following data acquisition, the DNA molecule is detected and collapsed into a one-dimensional (1D) image, containing the mean intensity value for each pixel along the extension of the molecule. The DNA molecule is detected for each individual time frame, and the obtained 1D images are stacked underneath each other, creating a *kymograph* (Figure 20). By detecting the edges of the DNA molecule for each time frame in the kymograph, the average extension can be calculated.

In order to extract the sequence specific information from the kymographs, molecule fluctuations, as well as drifting, inside the nanofluidic channels need to be considered. This is done by applying an algorithm, allowing the features of the kymograph to be aligned (123). In short, the edges are traced and shifted to the same position, ensuring that the extension of the molecule in each frame is the same. Next, the most pronounced bright,

or dark, feature, is detected and aligned by stretching each row in the kymograph separately. The newly aligned feature is fixed, and the process is repeated until the regions separating the fixed pixels are considered small enough. In order to obtain the final average intensity trace, referred to as a *barcode*, the mean value of each column in the aligned kymograph is calculated and plotted against the extension (Figure 20). In order to account for experimental differences in overall kymograph intensities, the intensity traces are normalized, with the average value set to 0, and standard deviation to 1.

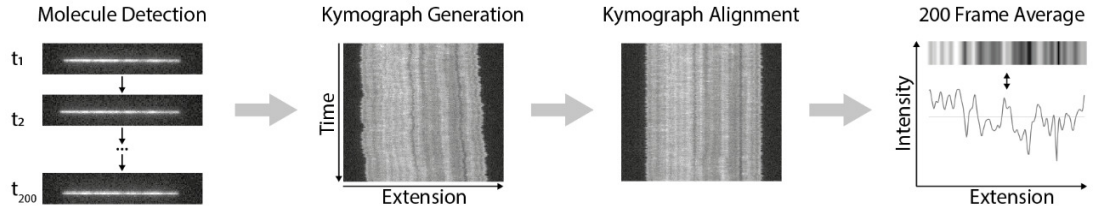

Figure 20: *Illustration of the main processing steps of the raw data. First, the molecule is detected in each individual time frame, where each frame is represented as a one-dimensional image containing the mean intensity along the extension of the molecule. The one-dimensional images are then stacked underneath each other in order to create a kymograph. The kymograph is aligned in order to account for molecule fluctuations and drifting inside the nanofluidic channels. Finally, the mean value is calculated for each column in the aligned kymograph, resulting in an average intensity trace along the extension of the molecule, which can serve as a fingerprint for plasmid identification.*

The barcode from each individual plasmid molecule can serve as a fingerprint of the underlying sequence. However, to remove any inconsistencies arising from experimental noise, barcodes originating from the same plasmid sequence can be averaged into a *consensus* barcode. When linearizing the circular plasmids (details in Section 4.2-4.4), the position of the double strand break can differ, causing the linear fragments to be circularly permutated. In order to account for a potential relative shift in the barcodes of two individual plasmids, a *cross-correlation* ($\hat{C}$) value is calculated.

The cross-correlation value puts a number on the similarity of two barcodes, where a value of +1 is the maximum, implying that the barcodes are identical, and a value of -1 is the minimum. The value is calculated by multiplying the intensity value of each pair of pixels from two individual barcodes, adding these together, and finally normalizing.

When comparing two barcodes, one will be fixed, and the other one shifted one pixel at the time, allowing the cross-correlation for each possible starting position to be calculated. Repeating the procedure for the flipped version of one of the barcodes enables the maximum cross-correlation for a pair of barcodes to be found.

The process of generating a consensus barcode can be seen in Figure 21. First, all barcodes are stretched to the same length, followed by calculating the maximum cross-correlation value for all possible pairs of barcodes. The two barcodes that display the highest cross-correlation value will then be merged at the position of the optimal shift, and possible flip, representing an average of the two individual barcodes. Next, the process is repeated, with the new average barcode replacing the two individual ones. Once again, the two barcodes showing the highest degree of similarity will be merged, and the process is repeated until only one consensus barcode remains.

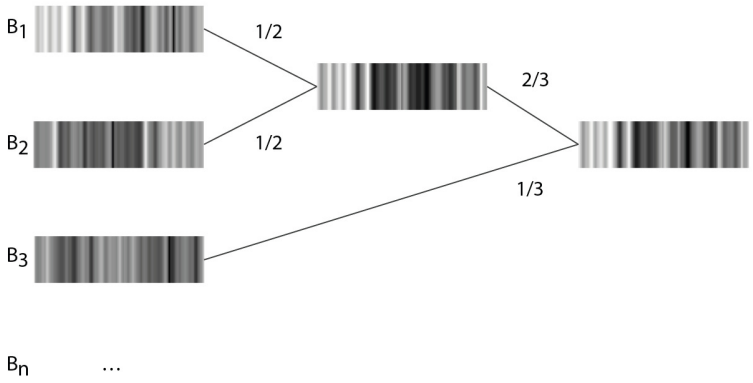

Figure 21: *Illustration of the process where individual barcodes are gradually merged, based on their degree of similarity, resulting in a final consensus barcode. The number at each line corresponds to the weight of the barcodes as they are merged.*

The obtained consensus barcodes were used to either identify a plasmid from a data base of previously sequenced plasmids (**Paper I**), or to trace the spread of a plasmid in an outbreak (**Paper II**). In order to enable the comparison of an *experimental* consensus barcode to known DNA sequences, *theoretical* barcodes were generated. Moreover, a statistical measure, termed *separability-score*, allowing to compare if a match to the

database was significant or not was defined. Similarly, a method for obtaining a statistical measure for the similarity between two experimental consensus barcodes was developed, rendering a *p-value* as output. Finally, in **Paper III**, a "*balls in boxes*" approach was used to determine if the maximum number of double strand breaks at a certain position along the plasmid contour could be deemed significant, allowing the presence of a resistance gene to be detected.

4.2 Identifying Plasmids from a Sequence Database

The aim of the study presented in **Paper I**, was to investigate the possibility to identify plasmids by comparing experimental barcodes to a database of theoretical barcodes. The previously established competitive binding protocol (112, 113), was adapted to plasmids, and evaluated using the three sequenced and well characterized plasmids, RP1 (60.1 kbp), R100 (94.3 kbp) and pUUH 239.2 (pUUH) (220.8 kbp), all encoding genes for antibiotic resistance. The circular nature of the plasmids provided both advantages, as well as challenges, when designing the assay. The ability to discriminate a circular plasmid from linear pieces of DNA (124, 125), ensured that only intact plasmid sequences were studied. However, in order to reveal the sequence specific pattern, the circular plasmids needed to be linearized. Using intense light exposure, reactive oxygen species were obtained (Section 4.1.1), capable of causing single strand breaks on the confined circular DNA. Once two singe stranded breaks occurred close enough to each other, the plasmid unfolded to its linear configuration.

To compare an experimental barcode to a DNA sequence, theoretical barcodes were generated (113). In short, the theory barcodes were created by considering the likelihood of YOYO and netropsin to bind a four bp site along the DNA sequence, and compensating for the resolution limit set by the experimental setup. Mainly, experimental consensus barcodes, generated from a number of individual barcodes, were used for the comparison with the theoretical barcodes from the database. Moreover, the consensus barcode of a plasmid was only compared to the plasmids from the database corresponding to a size of +/- 3 standard deviations (STD) from the experimentally measured size.

For the R100 plasmid, the experimental consensus barcode and the theory barcode showed a high degree of similarity, with a $\hat{C}$-value above 0.9 (Figure 22, left). When comparing the consensus barcode to all theory sequences of +/- 3 STD in size, two plasmids were clearly separated from the rest in terms of $\hat{C}$-value, R100 and NR1, where the latter is a variant of R100 with 99.8% sequence similarity (Figure 22, right).

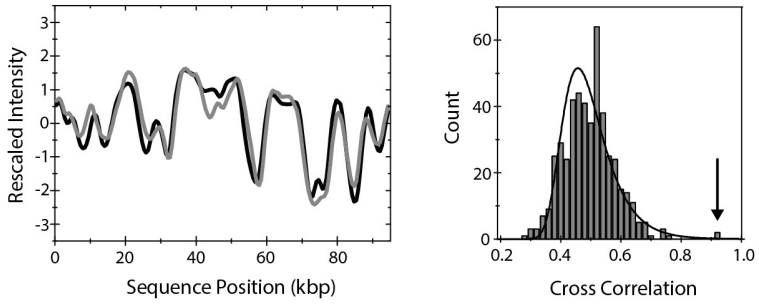

Figure 22: *Left: Comparison of the experimental consensus barcode (gray) of plasmid R100 with the corresponding theoretical barcode (black). Right: Histogram showing the best cross-correlation value obtained when comparing the experimental consensus barcode of R100 with all theoretical barcodes of +/- 3 STD in size from a database of all theoretical barcodes. The solid line corresponds to the Gumbel fit of the obtained data. The arrow indicates the cross-correlation value obtained for the correct sequence.*

For the shorter plasmid, RP1, a high degree of visual similarity, as well as a $\hat{C}$-value above 0.8, was obtained when comparing to the theoretical RP1 barcode. However, even if the $\hat{C}$ value for the correct sequence was in the top 0.005 fraction, it was not clearly separated from the rest of the theoretical barcodes. The lower separability of RP1 compared to R100 can be partially explained by the shorter sequence, resulting in a less unique barcode, as well as by the lower $\hat{C}$-value. For the third, and largest plasmid, pUUH, an inverted region of the sequence was found when comparing the consensus barcode with the theoretical barcode (Figure 23). Investigation of the DNA sequence revealed that the inverted region contained a cassette of resistance genes, flanked by transposable elements, capable of generating the inversion. The presence of the inversion was later confirmed with PCR. The $\hat{C}$-value of the consensus barcode compared to the theoretical barcode increased from 0.78 to 0.91, when correcting for the inverted sequence, clearly separating the correct sequence of the pUUH plasmid from the rest of the theoretical plasmid barcodes in the database.

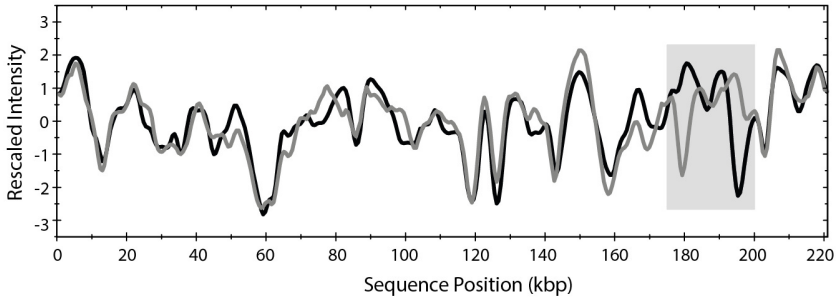

Figure 23: *Experimental consensus barcode (gray) compared to the theoretical barcode (black) for the plasmid pUUH 239.2. The gray box indicates the inverted region of the sequence.*

In order to generalize the results, an *in silico* comparison of all 3127 plasmids above 20 kbp from the NCBI RefSeq database, differing less than 20% in size, was made. A separability-score, similar to a traditional p-value, was introduced in order to provide a statistical significance for each well separated plasmid sequence. The results showed, using a separability-score of 0.01, that plasmids larger than about 70 kbp should be possible to identify using the assay, with an extreme lower limit of 30 kbp, depending on the uniqueness of the barcode.

In summary, **Paper I**, demonstrates that it is possible to identify clinically relevant plasmids by comparing experimental barcodes to a database of theoretical barcodes. The assay enables the intact sequence of individual plasmids to be studied and has the potential to detect structural variations.

4.3 Tracing Plasmids during an Outbreak

In contrast to **Paper I**, where the barcode of the plasmid was used for identification, we in **Paper II** investigated how the size of the plasmid, in combination with the barcode, could be used to trace plasmids originating from a nosocomial outbreak at Sahlgrenska University Hospital (126). Under the four month long outbreak in 2008, over 20 neonates were infected with multi-resistant bacteria, harboring extended spectrum beta-lactamase (ESBL) genes. The main strain of the outbreak was found to be an *E. coli* of sequence type (ST) 131 (126). However, two additional *E. coli* strains, ST73 and ST1444, were identified, as well as a *K. Pneumoniae* strain. Both *E. coli* and *K. Pneumoniae* belong to the family of

Enterobacteriaceae, which are well known to express ESBLs (70, 127, 128). Moreover, ESBL mediated resistance is frequently located on plasmids (129-131), thus the outbreak was suspected to be plasmid-born. However, it was not known if there in fact were multiple outbreaks occurring simultaneously, indicated by the presence of different types of bacterial strains and species, or if the outbreak was mediated by the transfer of a single plasmid between different bacteria.

The aim of the study presented in **Paper II** was to trace plasmids from the outbreak, by both monitoring plasmid content over time, and detecting the spread of plasmid between bacterial strains and species, as well as between patients. Unlike in **Paper I**, were experimental consensus barcodes of previously well characterized plasmids were compared to a database of theoretical barcodes, a method for comparing two experimental consensus barcodes with each other was developed in **Paper II**. In short, statistical information from all theoretical barcodes in the plasmid database was extracted. Based on this information, randomized barcodes were generated, acting as a reference model in order to convert the obtained $\hat{C}$-value, which is size dependent, to a p-value.

In total, 9 isolates, originating from 4 different neonates, were selected for the study, including isolates from all different strain types, as well as isolates sampled at different time points. The detected plasmids were characterized by size and barcode. The size of all the plasmids found in the 9 different isolates was obtained by measuring the extension of the plasmids in their circular form (124, 125), with results shown in Figure 24.

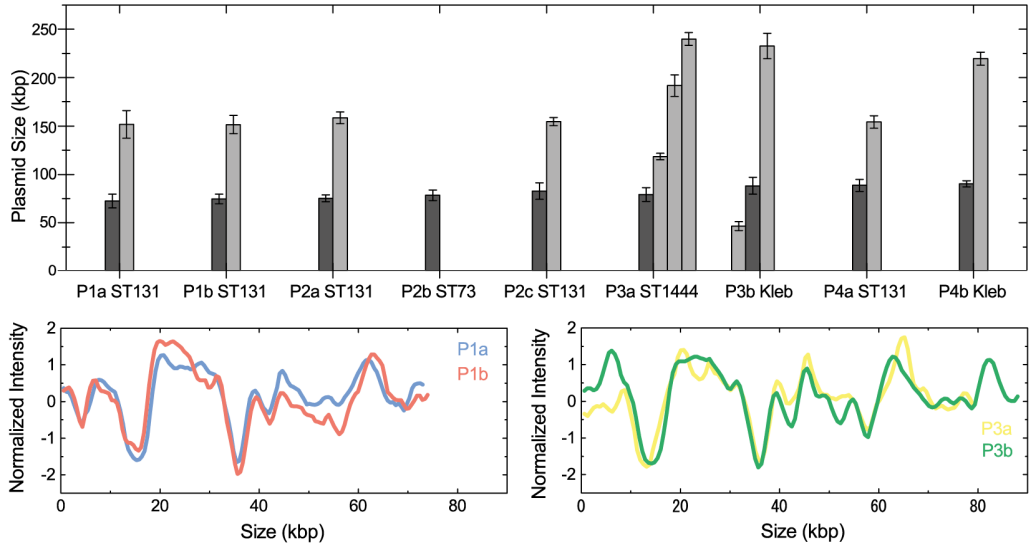

Figure 24: *Top: Histogram showing the measured size of each detected plasmid in the different isolates, including E. coli of strain types (ST) 131, 71 and 1444, as well as a strain of K. Pneumoniae (Kleb). The isolates are indexed by the patient number (PX) followed by a letter in order to discriminate isolates originating from the same patient. Bottom: Comparison of experimental consensus barcodes for the common plasmid found in isolate P1a and P1b, as well as P3a and P3b.*

The size measurements revealed a plasmid of similar size shared by all the isolates, ranging between 73-90 kbp in size, indicating that this plasmid was responsible for the spread of resistance. When studying the barcodes of the shared plasmid, they all showed a high degree of visual similarity. Moreover, by computing the p-value for all different pairs of plasmids, the results showed that the plasmids indeed displayed a statistically significant degree of similarity. Using the p-value tool when comparing two experimental consensus barcodes furthermore allowed the shared plasmid to be divided into two different subgroups, one displaying an extra insert at a specific position along the sequence, and one group without this insert (Figure 24). The extra piece in the DNA sequence in some of the plasmids also explains the differences in measured size. An overview of the findings when studying the plasmid content in all selected isolates can be seen in Figure 25.

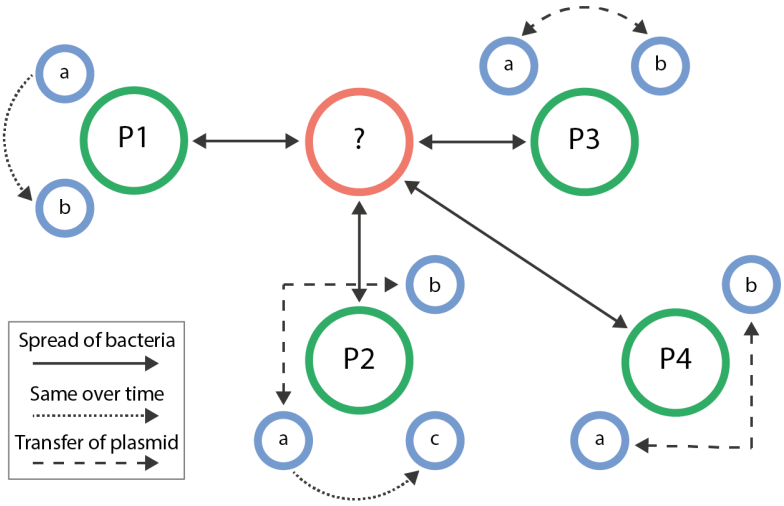

Figure 25: *Schematic illustration of the results obtained from the study presented in Paper II. Patients are represented by green circles, and individual isolates are shown in blue. The red circle corresponds to the unknown route of transmission.*

In summary, a shared plasmid of about 80 kbp in size with a highly similar barcode was found in each of the studied isolates, indicating that this plasmid was responsible for the spread of resistance. The results demonstrate the possibility of the assay to monitor plasmid content over time, detect the spread of plasmids between different bacteria strains and species, as well as indicating the transfer of bacteria between patients. The study shows how conclusions regarding the spread of resistance can be made, without knowing the sequence of the plasmid. Hence, the method shows great potential to provide guidance at an early stage during an outbreak situation, pinpointing which isolates that subsequently require a more detailed characterization.

4.4 Gene Detection

One of the main limitations of the assay presented in **Paper I-II**, was the inability to directly detect the presence of resistance genes. Using the outbreak studied in **Paper II** as an example, a modified assay allowing to pinpoint the resistance gene directly to the shared plasmid, in **Paper II** confirmed via subsequent PCR, would be highly desirable. Moreover, using the barcode to detect the presence of a resistance gene would not only

allow the assignment of the gene to a specific plasmid, but also to a precise location along the sequence.

With that goal in mind, **Paper III** demonstrated the development, and evaluation, of a novel assay for detecting resistance genes on single plasmids, utilizing the high sequence specificity of the Cas9 enzyme. By designing a crRNA sequence complementary to the gene of interest (Section 2.1.4), a plasmid harboring the gene will be "cut" at a specific location. Studying the positions of the double strand breaks along the barcodes of individual plasmids, enables determination of if a vast majority of the cuts have occurred at the same position along the sequence (Figure 26). By introducing a "balls in boxes" approach, the number of double strand breaks that by random chance would be expected to occur at the same position along the barcode can be simulated. A detection limit of + 3 STD of the obtained value enables the detection of a gene, provided that enough cuts have been observed at the same position.

In contrast to **Paper I-II**, circular plasmids were in **Paper III** not broken with light in order to reveal the barcode. Instead, circular plasmids were used solely for size determination, and pre-linearized plasmids were imaged in the nanochannels. For analysis, only linear fragments +/- 20% of the detected circular plasmids were analyzed, and the positions of the double strand breaks of the corresponding consensus barcodes were determined in order to detect the presence, or absence, of the gene of interest. In short, the number of linearized plasmids which encode the gene targeted by Cas9 will be high, consisting of mainly Cas9 cut plasmid molecules, but also include some which have been randomly linearized via mechanical stress or light exposure. In contrast, the number of fragments from a plasmid not harboring the targeted gene will be low, only containing randomly linearized plasmid molecules (Figure 26).

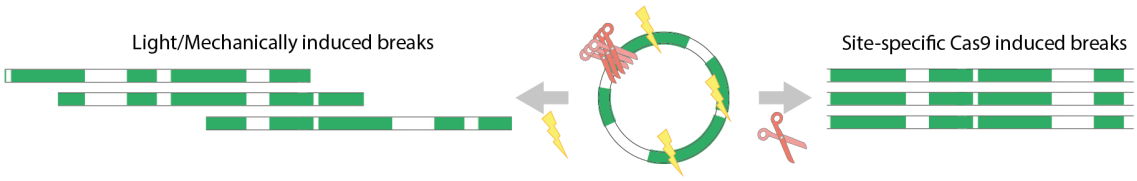

Figure 26: *Schematic illustration of the Cas9 assay. While a double strand break introduced by the Cas9 enzyme (red scissors), loaded with crRNA targeting the gene of interest, will be site specific, a break caused by light or mechanical stress (yellow lightning) will be randomly positioned along the contour of the plasmid. Hence, if the targeted gene is present (right), all linear fragments will have, within the experimental noise, identical barcodes. In contrast, if the targeted gene is not present (left), the linear fragments will be circularly permutated, broken only by light or mechanical stress.*

The principle of the assay was demonstrated on the previously sequenced plasmid pUUH, harboring the common ESBL gene *bla*$_{CTX\text{-}M\text{-}15}$. When adding crRNA with a sequence complementary to the *bla*$_{CTX\text{-}M\text{-}15}$ gene, a vast majority of the double strand breaks occurred at the predicted position along the sequence, thus confirming the presence of the gene. Similar results were obtained for other plasmid isolates, containing either one, or multiple plasmids, demonstrating the assays ability to not only detect the presence of resistance, but also to pinpoint it to a single plasmid.

As a final test, two previously uncharacterized plasmid isolates, DA28170 and D49173, were studied. Adding a cocktail consisting of two specifically designed crRNA molecules to the samples, it was possible to simultaneously target two of the main genes groups, *bla*$_{KPC}$ and *bla*$_{NDM}$, encoding for carbapenem resistance. For isolate DA49173, the results revealed the presence of two plasmids in the sample, where the smaller encoded the resistance (Figure 27). By subsequently testing each of the crRNAs separately, it could be concluded that the gene mediating the resistance belonged to the group of *bla*$_{KPC}$. Similarly, a *bla*$_{NDM}$ gene was detected on one of the plasmids found in isolate DA28170.

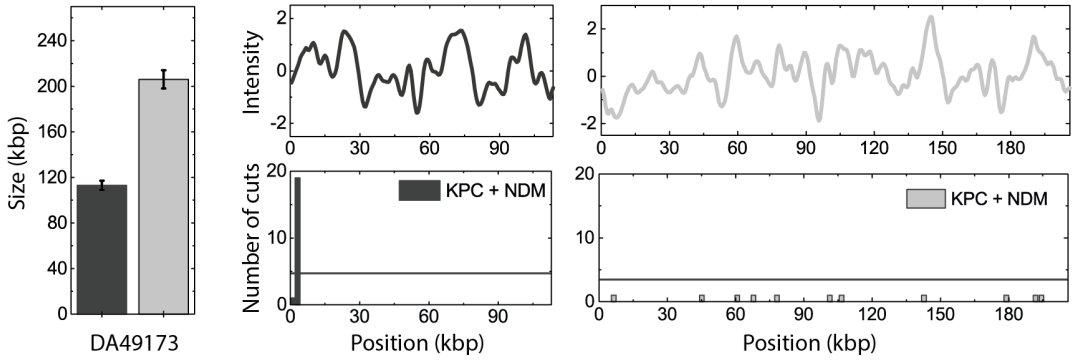

Figure 27: *Left: Sizes of the two plasmids found in isolate DA49173. The color of the bar indicates the presence (dark gray) or absence (light gray) of the resistance gene. Top Middle and Right: Experimental consensus barcodes of the smaller plasmid (dark gray) and larger plasmid (light gray) in isolate DA49173. Bottom Middle and Right: Histogram showing the location of double strand breaks along the contour of the small (dark gray) and large (light gray) plasmid when targeting the* bla_{KPC} *and* bla_{NDM} *gene families simultaneously. The horizontal lines in the histograms correspond to three standard deviations above the mean calculated value from the "balls in boxes" statistics. The results show that a majority of the double strand breaks occur at the same position along the sequence for the smaller plasmid found in the isolate, indicating the presence of a resistance gene.*

To summarize, with the progress presented in **Paper III,** the assay is capable of (i) detecting the size of all plasmids in a sample; (ii) providing a fingerprint which can be used for plasmid tracing or direct identification via a plasmid sequence database; and (iii) detecting the presence, or absence, of a (resistance) gene, assigning it to a precise position along a specific plasmid. Also, circumventing the need to manually break plasmids with light increases the speed of the method, as well as opens up for the possibility of future automatization.

5 Concluding Remarks and Outlook

With the rates of bacteria acquiring resistance to antibiotics drastically increasing throughout the world, new methods allowing to rapidly detect resistant bacteria will be of paramount importance. Resistance mainly spreads via horizontal gene transfer of mobile genetic elements, such as plasmids. Therefore, the primary focus of this Thesis has been to develop an assay specifically targeting bacterial plasmids.

The assay described in **Paper I-III** has allowed us to characterize plasmids based on size, their underlying DNA sequence, as well as enabled detection of resistance genes, even pinpointing the gene to a specific plasmid. The assay, based on optical DNA mapping, facilitates studies of plasmids at the single plasmid level, lowering the required amount of sample and allowing for investigation of structural variations. Competitive binding of YOYO and netropsin generates a sequence specific pattern along the DNA, which can be used both for tracing of plasmids, as well as for identification form a database of sequenced plasmids.

The developed assay provides a "birds-eye" view of the plasmid content in a sample and could either function as a complement to sequencing based strategies, or by its own for applications were bp resolution is not required. Compared to S1/PFGE, which provides information about plasmid size, the developed assay, following plasmid extraction, can be completed within hours instead of days. Moreover, the assay has the ability to separate plasmids of the same size based on their barcode. Similar to PCR-based techniques for plasmid characterization, the progress in **Paper III** now allows the developed assay to target specific genes. However, in contrast to PCR-based techniques, the developed assay can pinpoint which particular plasmid in the sample that harbors the gene of interest. Moreover, if the targeted gene is not present, PCR-based methods would not reveal any information about the plasmid content of the sample, while the assay presented in the Thesis would still provide details of plasmid size and the corresponding barcode.

Even if the developed assay in its current format provides important insights when studying plasmids, several key points still need to be addressed in order for the assay to function as a reliable tool for POC diagnostics. For the studies presented in the Thesis, all plasmid samples have been extracted from pre-cultivated bacteria, drastically increasing the lead time of the assay, thus reducing the potential impact in clinical settings. However, since the required amount of sample for the developed assay is very low, the need for cultivation could likely be significantly decreased. Refining the assay to simultaneously detect and characterize chromosomal fragments, would make the method more versatile, allowing for detection of resistance mediated by the chromosome and plasmids at the same time. Moreover, there would be no need for separating the plasmid DNA from the chromosomal DNA, simplifying the process of extracting DNA form uncultivated bacteria. Ways of increasing the resolution of the assay to efficiently target plasmids of sizes below 40 kbp, would furthermore be desirable.

Based on the work presented in the Thesis, current efforts include (i) simplifying data acquisition using a custom built smartphone based fluorescence microscope, enabling the detection of resistance gene in remote resource limited POC settings; (ii) using the experimental consensus barcode as a template for assembling reads obtained from DNA sequencing; (iii) fabricating nanofluidic chips that permit analysis of multiple isolates in parallel; (iv) characterizing chromosomal and plasmid DNA simultaneously; and (v), in collaboration with microbiologists at Uppsala University, studying DNA from low concentration samples extracted directly form uncultivated bacteria.

Even if the resolution of the assay could potentially be improved by the use of more advanced optics and imaging techniques, it will never be able to compete with the bp resolution provided by DNA sequencing. Instead, efforts to decrease the cost, as well as increasing the speed and simplicity of the assay are the main focus. Moreover, there is the possibility to add sequence specific marks along the DNA in order to increase the uniqueness of the barcode. One such example is pinpointing the position of a resistance gene, as demonstrated in **Paper III**. Using **Paper I** as an example, the possibility to identify a plasmid from the database of theoretical sequences could be significantly increased by (i) removing all theoretical barcodes not containing the 23bp site targeted by Cas9; and (ii) adjusting the method of calculating the $\hat{C}$-values, lowering the overall score for non-matching barcodes. Hence, the size limit for a plasmid to obtain a unique match against the database should decrease significantly.

In a recent paper, we describe how a filtering method enables the use of plasmid barcodes from only a single time frame (132), circumventing the need of averaging. Together with the progress made in **Paper III**, were plasmids no longer are linearized with light, the filtering methods is a key stepping stone towards turning the assay into a high throughput application. Moreover, single time frames, in combination with the competitive binding assay, has the potential to be used for mapping of large sets of DNA, such as the human genome.

To conclude, the assay developed in **Paper I-III** provides information about the biology of plasmids and shows great potential as a first step of plasmid characterization. In order for the assay to be a reliable alternative as a POC diagnostics tool, a few key issues still remain to be solved. Yet, the assay in its current format provides useful insights on plasmids and how they spread, information which is highly desirable in the battle against antibiotic resistance.

6 Acknowledgements

I would like to sincerely thank the following people for their direct or indirect support.

My supervisor, **Fredrik Westerlund** for all your support, encouragement and commitment. It is a great joy working together with you.

My boss **Pernilla Wittung Stafshede** for your positive energy, passion for science and strong leadership.

My co-supervisor **Ivan Mijakovic** for discussions and support.

Lena Nyberg for teaching me all the secrets in the lab, providing endless support and for proof reading the Thesis.

Members of the Westerlund group; **Karolin Frykholm, Mohammadreza Alizadehheidari**, **Robin Öz**, **Santosh Kumar Bikarolla, Sriram K. K.**, **Sune Levin**, **Kai Jiang and Vandana Singh**.

Tobias Ambjörnsson and his research group at Lund University, especially **Saair Quaderi**, **Christoffer Pichler**, **Paola Torche Pedreschi** and **Albertas Dvirnas**. Thanks for all the amazing work on the data analysis software and for responding to all my endless lists via email.

The experts on plasmids and antibiotic resistance, especially **Nahid Karami** and **Tinna Åhrén** from Sahlgrenska Academy**, Linus Sandegren** and **Fredrik Rajer** from Uppsala University and **Erik Kristiansson** from Chalmers. Thanks for all the interesting discussions and for sharing your knowledge.

All additional **co-authors** for interesting collaborations.

My roommates **Hoda**, **Jesper**, **Sangamesh** and **Pegah**. Thank you for the laughs.

My mentors **David**, **Jesper** and **Lena**.

All **colleagues** at Chemical Biology and Physical Chemistry for the friendly atmosphere.

Finally, **Sanna** and **Stella** for always reminding me that there are more important things in life than work.

7 References

1. Fleming A. On the Antibacterial Action of Cultures of a Penicillium, with Special Reference to their Use in the Isolation of B. influenzæ. British journal of experimental pathology. 1929;10(3):226-36.

2. Chain E, Florey HW, Adelaide MB, Gardner AD, Heatley NG, Jennings MA, et al. Penicillin as a chemoterapeutic agent. The Lancet Infectious Diseases. 2014;236(6104):226-8.

3. The Review on Antimicrobial Resistance. Tackling drug-resistant infections globally: final report and recommendations. 2016.

4. World Health Organization. Antimicrobial resistance: global report on surveillance. 2014.

5. Livermore DM, Wain J. Revolutionising bacteriology to improve treatment outcomes and antibiotic stewardship. Infection & chemotherapy. 2013;45(1):1-10.

6. Frost LS, Leplae R, Summers AO, Toussaint A. Mobile genetic elements: the agents of open source evolution. Nature reviews Microbiology. 2005;3(9):722-32.

7. Smillie C, Garcillán-Barcia MP, Francia MV, Rocha EPC, de la Cruz F. Mobility of Plasmids. Microbiology and Molecular Biology Reviews. 2010;74(3):434-52.

8. Carattoli A. Plasmids and the spread of resistance. International journal of medical microbiology. 2013;303(6-7):298-304.

9. Barton BM, Harding GP, Zuccarelli AJ. A general method for detecting and sizing large plasmids. Analytical biochemistry. 1995;226(2):235-40.

10. Carattoli A. Plasmids in Gram negatives: molecular typing of resistance plasmids. International journal of medical microbiology. 2011;301(8):654-8.

11. Heather JM, Chain B. The sequence of sequencers: The history of sequencing DNA. Genomics. 2016;107(1):1-8.

12. Brolund A, Sandegren L. Characterization of ESBL disseminating plasmids. Infectious diseases. 2016;48(1):18-25.

13. Köser CU, Ellington MJ, Peacock SJ. Whole-genome sequencing to control antimicrobial resistance. Trends in Genetics. 2014;30(9):401-7.

14. Schwartz DC, Li X, Hernandez LI, Ramnarain SP, Huff EJ, Wang YK. Ordered restriction maps of Saccharomyces cerevisiae chromosomes constructed by optical mapping. Science. 1993;262(5130):110-4.

15. Neely RK, Deen J, Hofkens J. Optical mapping of DNA: single-molecule-based methods for mapping genomes. Biopolymers. 2011;95(5):298-311.

16. Levy-Sakin M, Ebenstein Y. Beyond sequencing: optical mapping of DNA in the age of nanotechnology and nanoscopy. Current opinion in biotechnology. 2013;24(4):690-8.

17. Avery OT, MacLeod CM, McCarty M. Studies on the chemical nature of the substance inducing transformation of pneumococcal types: induction of transformation by a desoxyribonucleic acid fraction isolated from pneumococcus typE III. The Journal of Experimental Medicine. 1944;79(2):137-58.

18. Watson JD, Crick FH. Molecular structure of nucleic acids; a structure for deoxyribose nucleic acid. Nature. 1953;171(4356):737-8.

19. Watson JD, Crick FH. Genetical implications of the structure of deoxyribonucleic acid. Nature. 1953;171:964-7.

20. Bloomfield VAC, Donald M., Tinoco I. Nucleic Acids: Structure, Properties, and Functions: University Science Books; 2000.

21. Crick FH. On protein synthesis. Symposia of the Society for Experimental Biology. 1958;12:138-63.

22. Crick FH. Central dogma of molecular biology. Nature. 1970;227(5258):561-3.

23. Reisner W, Pedersen JN, Austin RH. DNA confinement in nanochannels: physics and biological applications. Reports on progress in physics. 2012;75(10):106601.

24. Baumann CG, Smith SB, Bloomfield VA, Bustamante C. Ionic effects on the elasticity of single DNA molecules. Proceedings of the National Academy of Sciences of the United States of America. 1997;94(12):6185-90.

25. Daoud M, De Gennes PG. Statistics of macromolecular solutions trapped in small pores. J Phys France. 1977;38(1):85-93.

26. Odijk T. The statistics and dynamics of confined or entangled stiff polymers. Macromolecules. 1983;16(8):1340-4.

27. Odijk T. Similarity applied to the statistics of confined stiff polymers. Macromolecules. 1984;17(3):502-3.

28. Tree DR, Wang Y, Dorfman KD. Mobility of a semiflexible chain confined in a nanochannel. Physical review letters. 2012;108(22):228105.

29. Wang Y, Tree DR, Dorfman KD. Simulation of DNA Extension in Nanochannels. Macromolecules. 2011;44(16):6594-604.

30. Werner E, Mehlig B. Confined polymers in the extended de Gennes regime. Physical review E. 2014;90(6):062602.

31. Iarko V, Werner E, Nyberg LK, Muller V, Fritzsche J, Ambjornsson T, et al. Extension of nanoconfined DNA: Quantitative comparison between experiment and theory. Physical review E. 2015;92(6):062701.

32. Gupta D, Miller JJ, Muralidhar A, Mahshid S, Reisner W, Dorfman KD. Experimental Evidence of Weak Excluded Volume Effects for Nanochannel Confined DNA. ACS Macro Letters. 2015;4(7):759-63.

33. Rye HS, Yue S, Wemmer DE, Quesada MA, Haugland RP, Mathies RA, et al. Stable fluorescent complexes of double-stranded DNA with bis-intercalating asymmetric cyanine dyes: properties and applications. Nucleic Acids Research. 1992;20(11):2803-12.

34. Larsson A, Carlsson C, Jonsson M, Albinsson B. Characterization of the Binding of the Fluorescent Dyes YO and YOYO to DNA by Polarized Light Spectroscopy. Journal of the American Chemical Society. 1994;116(19):8459-65.

35. Paik DH, Perkins TT. Dynamics and Multiple Stable Binding Modes of DNA Intercalators Revealed by Single-Molecule Force Spectroscopy. Angewandte Chemie International Edition. 2012;51(8):1811-5.

36. Gunther K, Mertig M, Seidel R. Mechanical and structural properties of YOYO-1 complexed DNA. Nucleic Acids Research. 2010;38(19):6526-32.

37. Berman HM, Neidle S, Zimmer C, Thrum H. Netropsin, a DNA-binding oligopeptide structural and binding studies. Biochim Biophys Acta. 1979;561(1):124-31.

38. Bailly C, Chaires JB. Sequence-specific DNA minor groove binders. Design and synthesis of netropsin and distamycin analogues. Bioconjugate chemistry. 1998;9(5):513-38.

39. Marky LA, Breslauer KJ. Origins of netropsin binding affinity and specificity: correlations of thermodynamic and structural data. Proceedings of the National Academy of Sciences of the United States of America. 1987;84(13):4359-63.

40. Boger DL, Fink BE, Brunette SR, Tse WC, Hedrick MP. A Simple, High-Resolution Method for Establishing DNA Binding Affinity and Sequence Selectivity. Journal of the American Chemical Society. 2001;123(25):5878-91.

41. Zimmer C, Marck C, Schneider C, Guschlbauer W. Influence of nucleotide sequence on dA.dT-specific binding of Netropsin to double stranded DNA. Nucleic Acids Research. 1979;6(8):2831-7.

42. Horvath P, Barrangou R. CRISPR/Cas, the immune system of bacteria and archaea. Science. 2010;327(5962):167-70.

43. Marraffini LA, Sontheimer EJ. CRISPR interference: RNA-directed adaptive immunity in bacteria and archaea. Nat Rev Genetics. 2010;11(3):181-90.

44. Jinek M, Chylinski K, Fonfara I, Hauer M, Doudna JA, Charpentier E. A programmable dual-RNA-guided DNA endonuclease in adaptive bacterial immunity. Science. 2012;337(6096):816-21.

45. Cong L, Ran FA, Cox D, Lin S, Barretto R, Habib N, et al. Multiplex Genome Engineering Using CRISPR/Cas Systems. Science. 2013;339(6121):819-23.

46. Rath D, Amlinger L, Rath A, Lundgren M. The CRISPR-Cas immune system: biology, mechanisms and applications. Biochimie. 2015;117:119-28.

47. Sander JD, Joung JK. CRISPR-Cas systems for editing, regulating and targeting genomes. Nature biotechnology. 2014;32(4):347-55.

48. Maeder ML, Linder SJ, Cascio VM, Fu Y, Ho QH, Joung JK. CRISPR RNA-guided activation of endogenous human genes. Nature methods. 2013;10(10):977-9.

49. Chen B, Gilbert LA, Cimini BA, Schnitzbauer J, Zhang W, Li G-W, et al. Dynamic Imaging of Genomic Loci in Living Human Cells by an Optimized CRISPR/Cas System. Cell. 2013;155(7):1479-91.

50. Anton T, Bultmann S, Leonhardt H, Markaki Y. Visualization of specific DNA sequences in living mouse embryonic stem cells with a programmable fluorescent CRISPR/Cas system. Nucleus (Austin, Tex). 2014;5(2):163-72.

51. Koike-Yusa H, Li Y, Tan EP, Velasco-Herrera Mdel C, Yusa K. Genome-wide recessive genetic screening in mammalian cells with a lentiviral CRISPR-guide RNA library. Nature biotechnology. 2014;32(3):267-73.

52. McCaffrey J, Sibert J, Zhang B, Zhang Y, Hu W, Riethman H, et al. CRISPR-CAS9 D10A nickase target-specific fluorescent labeling of double strand DNA for whole genome mapping and structural variation analysis. Nucleic Acids Research. 2016;44(2):e11.

53. Wassenaar TM. Bacteria: The Benign, the Bad, and the Beautiful: Wiley-Blackwell; 2011.

54. Lederberg J. Cell genetics and hereditary symbiosis. Physiological reviews. 1952;32(4):403-30.

55. Novick RP. Plasmid incompatibility. Microbiological reviews. 1987;51(4):381-95.

56. Madigan MTM, John M, Brock TD. Brock - Biology of Microorganisms: Pearson Prentice Hall; 2006.

57. Srivastava S. Genetics of Bacteria: Springer; 2013.

58. Sandegren L, Andersson DI. Bacterial gene amplification: implications for the evolution of antibiotic resistance. Nature reviews Microbiology. 2009;7(8):578-88.

59. Germond J-E, Vogt VM, Hirt B. Characterization of the Single-Strand-Specific Nuclease S1 Activity on Double-Stranded Supercoiled Polyoma DNA. European Journal of Biochemistry. 1974;43(3):591-600.

60. Mullis K, Faloona F, Scharf S, Saiki R, Horn G, Erlich H. Specific enzymatic amplification of DNA in vitro: the polymerase chain reaction. Cold Spring Harbor symposia on quantitative biology. 1986;51:263-73.

61. Heid CA, Stevens J, Livak KJ, Williams PM. Real time quantitative PCR. Genome research. 1996;6(10):986-94.

62. Carattoli A, Bertini A, Villa L, Falbo V, Hopkins KL, Threlfall EJ. Identification of plasmids by PCR-based replicon typing. Journal of microbiological methods. 2005;63(3):219-28.

63. Garcia-Fernandez A, Chiaretto G, Bertini A, Villa L, Fortini D, Ricci A, et al. Multilocus sequence typing of IncI1 plasmids carrying extended-spectrum beta-lactamases in Escherichia coli and Salmonella of human and animal origin. The Journal of antimicrobial chemotherapy. 2008;61(6):1229-33.

64. Metzker ML. Sequencing technologies - the next generation. Nat Rev Genetics. 2010;11(1):31-46.

65. Bahassi el M, Stambrook PJ. Next-generation sequencing technologies: breaking the sound barrier of human genetics. Mutagenesis. 2014;29(5):303-10.

66. Shendure J, Ji H. Next-generation DNA sequencing. Nature biotechnology. 2008;26(10):1135-45.

67. Eid J, Fehr A, Gray J, Luong K, Lyle J, Otto G, et al. Real-time DNA sequencing from single polymerase molecules. Science. 2009;323(5910):133-8.

68. Conlan S, Thomas PJ, Deming C, Park M, Lau AF, Dekker JP, et al. Single-molecule sequencing to track plasmid diversity of hospital-associated carbapenemase-producing Enterobacteriaceae. Science translational medicine. 2014;6(254):126.

69. Czaplewski L, Bax R, Clokie M, Dawson M, Fairhead H, Fischetti VA, et al. Alternatives to antibiotics - a pipeline portfolio review. The Lancet Infectious Diseases. 2016;16(2):239-51.

70. Nordmann P, Dortet L, Poirel L. Carbapenem resistance in Enterobacteriaceae: here is the storm! Trends in molecular medicine. 2012;18(5):263-72.

71. Liu Y-Y, Wang Y, Walsh TR, Yi L-X, Zhang R, Spencer J, et al. Emergence of plasmid-mediated colistin resistance mechanism MCR-1 in animals and human beings in China: a microbiological and molecular biological study. The Lancet Infectious Diseases. 2016;16(2):161-8.

72. Blair JMA, Webber MA, Baylay AJ, Ogbolu DO, Piddock LJV. Molecular mechanisms of antibiotic resistance. Nature reviews Microbiology. 2015;13(1):42-51.

73. Dantas G, Sommer MAO. How to Fight Back Against Antibiotic Resistance. American Scientist. 2014;102(1):42-51.

74. Cho H, Uehara T, Bernhardt TG. Beta-lactam antibiotics induce a lethal malfunctioning of the bacterial cell wall synthesis machinery. Cell. 2014;159(6):1300-11.

75. Sorensen SJ, Bailey M, Hansen LH, Kroer N, Wuertz S. Studying plasmid horizontal transfer in situ: a critical review. Nature reviews Microbiology. 2005;3(9):700-10.

76. Funnell BE, Phillips GJ. Plasmid Biology: ASM Press; 2004.

77. Persson F, Tegenfeldt JO. DNA in nanochannels-directly visualizing genomic information. Chemical Society Reviews. 2010;39(3):985-99.

78. Levy SL, Craighead HG. DNA manipulation, sorting, and mapping in nanofluidic systems. Chemical Society Reviews. 2010;39(3):1133-52.

79. Friedrich SM, Zec HC, Wang T-H. Analysis of single nucleic acid molecules in micro- and nano-fluidics. Lab on a Chip. 2016;16(5):790-811.

80. Marie R, Kristensen A. Nanofluidic devices towards single DNA molecule sequence mapping. Journal of biophotonics. 2012;5(8-9):673-86.

81. Muller V, Westerlund F. Optical DNA mapping in nanofluidic devices: principles and applications. Lab on a Chip. 2017;17(4):579-90.

82. Bensimon A, Simon A, Chiffaudel A, Croquette V, Heslot F, Bensimon D. Alignment and sensitive detection of DNA by a moving interface. Science. 1994;265(5181):2096-8.

83. Michalet X, Ekong R, Fougerousse F, Rousseaux S, Schurra C, Hornigold N, et al. Dynamic molecular combing: stretching the whole human genome for high-resolution studies. Science. 1997;277(5331):1518-23.

84. Tegenfeldt JO, Prinz C, Cao H, Chou S, Reisner WW, Riehn R, et al. The dynamics of genomic-length DNA molecules in 100-nm channels. Proceedings of the National Academy of Sciences of the United States of America. 2004;101(30):10979-83.

85. Jo K, Dhingra DM, Odijk T, de Pablo JJ, Graham MD, Runnheim R, et al. A single-molecule barcoding system using nanoslits for DNA analysis. Proceedings of the National Academy of Sciences of the United States of America. 2007;104(8):2673-8.

86. Das SK, Austin MD, Akana MC, Deshpande P, Cao H, Xiao M. Single molecule linear analysis of DNA in nano-channel labeled with sequence specific fluorescent probes. Nucleic Acids Research. 2010;38(18):e177.

87. Hastie AR, Dong L, Smith A, Finklestein J, Lam ET, Huo N, et al. Rapid Genome Mapping in Nanochannel Arrays for Highly Complete and Accurate De Novo Sequence Assembly of the Complex Aegilops tauschii Genome. PLoS ONE. 2013;8(2):e55864.

88. Pendleton M, Sebra R, Pang AW, Ummat A, Franzen O, Rausch T, et al. Assembly and diploid architecture of an individual human genome via single-molecule technologies. Nat Methods. 2015;12(8):780-6.

89. Mostovoy Y, Levy-Sakin M, Lam J, Lam ET, Hastie AR, Marks P, et al. A hybrid approach for de novo human genome sequence assembly and phasing. Nat Methods. 2016;13(7):587-90.

90. Lam ET, Hastie A, Lin C, Ehrlich D, Das SK, Austin MD, et al. Genome mapping on nanochannel arrays for structural variation analysis and sequence assembly. Nature biotechnology. 2012;30(8):771-6.

91. Xiao S, Li J, Ma F, Fang L, Xu S, Chen W, et al. Rapid construction of genome map for large yellow croaker (Larimichthys crocea) by the whole-genome mapping in BioNano Genomics Irys system. BMC genomics. 2015;16:670.

92. Usher CL, Handsaker RE, Esko T, Tuke MA, Weedon MN, Hastie AR, et al. Structural forms of the human amylase locus and their relationships to SNPs, haplotypes and obesity. Nature genetics. 2015;47(8):921-5.

93. VanBuren R, Bryant D, Edger PP, Tang H, Burgess D, Challabathula D, et al. Single-molecule sequencing of the desiccation-tolerant grass Oropetium thomaeum. Nature. 2015;527(7579):508-11.

94. Yang J, Liu D, Wang X, Ji C, Cheng F, Liu B, et al. The genome sequence of allopolyploid Brassica juncea and analysis of differential homoeolog gene expression influencing selection. Nature genetics. 2016;48(10):1225-32.

95. Chaney L, Sharp AR, Evans CR, Udall JA. Genome Mapping in Plant Comparative Genomics. Trends in plant science. 2016;21(9):770-80.

96. Martin G, Baurens F-C, Droc G, Rouard M, Cenci A, Kilian A, et al. Improvement of the banana "Musa acuminata" reference sequence using NGS data and semi-automated bioinformatics methods. BMC genomics. 2016;17(1):243.

97. Mak AC, Lai YY, Lam ET, Kwok TP, Leung AK, Poon A, et al. Genome-Wide Structural Variation Detection by Genome Mapping on Nanochannel Arrays. Genetics. 2016;202(1):351-62.

98. Shi L, Guo Y, Dong C, Huddleston J, Yang H, Han X, et al. Long-read sequencing and de novo assembly of a Chinese genome. Nature communications. 2016;7:12065.

99. Rosenfeld JA, Reeves D, Brugler MR, Narechania A, Simon S, Durrett R, et al. Genome assembly and geospatial phylogenomics of the bed bug Cimex lectularius. Nature communications. 2016;7:10164.

100. Klimasauskas S, Weinhold E. A new tool for biotechnology: AdoMet-dependent methyltransferases. Trends in biotechnology. 2007;25(3):99-104.

101. Lukinavičius G, Lapienė V, Staševskij Z, Dalhoff C, Weinhold E, Klimašauskas S. Targeted Labeling of DNA by Methyltransferase-Directed Transfer of Activated Groups (mTAG). Journal of the American Chemical Society. 2007;129(10):2758-9.

102. Vranken C, Deen J, Dirix L, Stakenborg T, Dehaen W, Leen V, et al. Super-resolution optical DNA Mapping via DNA methyltransferase-directed click chemistry. Nucleic Acids Research. 2014;42(7):e50-e.

103. Grunwald A, Dahan M, Giesbertz A, Nilsson A, Nyberg LK, Weinhold E, et al. Bacteriophage strain typing by rapid single molecule analysis. Nucleic Acids Research. 2015;43(18):e117.

104. Lim SF, Karpusenko A, Sakon JJ, Hook JA, Lamar TA, Riehn R. DNA methylation profiling in nanochannels. Biomicrofluidics. 2011;5(3):34106-341068.

105. Levy-Sakin M, Grunwald A, Kim S, Gassman NR, Gottfried A, Antelman J, et al. Toward single-molecule optical mapping of the epigenome. ACS nano. 2014;8(1):14-26.

106. Michaeli Y, Shahal T, Torchinsky D, Grunwald A, Hoch R, Ebenstein Y. Optical detection of epigenetic marks: sensitive quantification and direct imaging of individual hydroxymethylcytosine bases. Chemical Communications. 2013;49(77):8599-601.

107. Lim SF, Karpusenko A, Blumers AL, Streng DE, Riehn R. Chromatin modification mapping in nanochannels. Biomicrofluidics. 2013;7(6):64105.

108. Zirkin S, Fishman S, Sharim H, Michaeli Y, Don J, Ebenstein Y. Lighting up individual DNA damage sites by in vitro repair synthesis. Journal of the American Chemical Society. 2014;136(21):7771-6.

109. Reisner W, Larsen NB, Silahtaroglu A, Kristensen A, Tommerup N, Tegenfeldt JO, et al. Single-molecule denaturation mapping of DNA in nanofluidic channels. Proceedings of the National Academy of Sciences of the United States of America. 2010;107(30):13294-9.

110. Welch RL, Sladek R, Dewar K, Reisner WW. Denaturation mapping of Saccharomyces cerevisiae. Lab on a Chip. 2012;12(18):3314-21.

111. Marie R, Pedersen JN, Bauer DL, Rasmussen KH, Yusuf M, Volpi E, et al. Integrated view of genome structure and sequence of a single DNA molecule in a nanofluidic device. Proceedings of the National Academy of Sciences of the United States of America. 2013;110(13):4893-8.

112. Nyberg LK, Persson F, Berg J, Bergstrom J, Fransson E, Olsson L, et al. A single-step competitive binding assay for mapping of single DNA molecules. Biochemical and biophysical research communications. 2012;417(1):404-8.

113. Nilsson AN, Emilsson G, Nyberg LK, Noble C, Stadler LS, Fritzsche J, et al. Competitive binding-based optical DNA mapping for fast identification of bacteria--multi-ligand transfer matrix theory and experimental applications on Escherichia coli. Nucleic Acids Research. 2014;42(15):e118.

114. Kasha M. Characterization of electronic transitions in complex molecules. Discussions of the Faraday Society. 1950;9(0):14-9.

115. Lakowicz JR. Principles of Fluorescence Spectroscopy: Springer; 2006.

116. Dorfman KD, King SB, Olson DW, Thomas JDP, Tree DR. Beyond Gel Electrophoresis: Microfluidic Separations, Fluorescence Burst Analysis, and DNA Stretching. Chemical Reviews. 2013;113(4):2584-667.

117. Persson F, Utko P, Reisner W, Larsen NB, Kristensen A. Confinement spectroscopy: probing single DNA molecules with tapered nanochannels. Nano letters. 2009;9(4):1382-5.

118. Freitag C, Noble C, Fritzsche J, Persson F, Reiter-Schad M, Nilsson AN, et al. Visualizing the entire DNA from a chromosome in a single frame. Biomicrofluidics. 2015;9(4):044114.

119. Persson F, Fritzsche J, Mir KU, Modesti M, Westerlund F, Tegenfeldt JO. Lipid-Based Passivation in Nanofluidics. Nano letters. 2012;12(5):2260-5.

120. Duan C, Wang W, Xie Q. Review article: Fabrication of nanofluidic devices. Biomicrofluidics. 2013;7(2):26501.

121. Nyberg L, Persson F, Åkerman B, Westerlund F. Heterogeneous staining: a tool for studies of how fluorescent dyes affect the physical properties of DNA. Nucleic Acids Research. 2013;41(19):e184-e.

122. Akerman B, Tuite E. Single- and double-strand photocleavage of DNA by YO, YOYO and TOTO. Nucleic Acids Research. 1996;24(6):1080-90.

123. Noble C, Nilsson AN, Freitag C, Beech JP, Tegenfeldt JO, Ambjörnsson T. A Fast and Scalable Kymograph Alignment Algorithm for Nanochannel-Based Optical DNA Mappings. PLoS ONE. 2015;10(4):e0121905.

124. Frykholm K, Nyberg LK, Lagerstedt E, Noble C, Fritzsche J, Karami N, et al. Fast size-determination of intact bacterial plasmids using nanofluidic channels. Lab on a Chip. 2015;15(13):2739-43.

125. Alizadehheidari M, Werner E, Noble C, Reiter-Schad M, Nyberg LK, Fritzsche J, et al. Nanoconfined Circular and Linear DNA: Equilibrium Conformations and Unfolding Kinetics. Macromolecules. 2015;48(3):871-8.

126. Karami N, Helldal L, Welinder-Olsson C, Åhrén C, Moore ERB. Sub-Typing of Extended-Spectrum-β-Lactamase-Producing Isolates from a Nosocomial Outbreak: Application of a 10-Loci Generic Escherichia coli Multi-Locus Variable Number Tandem Repeat Analysis. PLoS ONE. 2014;8(12):e83030.

127. Paterson DL. Resistance in gram-negative bacteria: enterobacteriaceae. The American journal of medicine. 2006;119(6):S20-8.

128. Bush K. Alarming beta-lactamase-mediated resistance in multidrug-resistant Enterobacteriaceae. Current opinion in microbiology. 2010;13(5):558-64.

129. Mathers AJ, Peirano G, Pitout JD. The role of epidemic resistance plasmids and international high-risk clones in the spread of multidrug-resistant Enterobacteriaceae. Clinical microbiology reviews. 2015;28(3):565-91.

130. Carattoli A. Resistance plasmid families in Enterobacteriaceae. Antimicrobial agents and chemotherapy. 2009;53(6):2227-38.

131. Schultsz C, Geerlings S. Plasmid-mediated resistance in Enterobacteriaceae: changing landscape and implications for therapy. Drugs. 2012;72(1):1-16.

132. Torche PC, Muller V, Westerlund F, Ambjornsson T. Noise reduction in single time frame optical DNA maps. PLoS ONE. 2017;12(6):e0179041.